THE JOURNAL OF THE INSTITUTION OF ENGINEERS, MALAYSIA KDN PP5476/10/2012 (030203) | ISSN 0126-513X

IEM JOURNAL

VOL. 83, NO. 1
JUNE 2022

IEM
The Institution of Engineers, Malaysia

Vol. 83, No. 1, June 2022
KDN PP5476/10/2012 (030203) ISSN 0126-513X

CONTENTS

THIS ISSUE WAS PUBLISHED IN JULY 2023

THE INSTITUTION OF ENGINEERS, MALAYSIA
Bangunan Ingenieur, Lots 60 & 62, Jalan 52/4,
P.O.Box 223 (Jalan Sultan),
46720 Petaling Jaya, Selangor Darul Ehsan.
Tel: 03-7968 4001/4002
Fax: 03-7957 7678
E-mail: sec@iem.org.my **Homepage:** http://www.myiem.org.my

PRINT QUANTITY: *500 COPIES*

LIGHTNING SHIELDING WITH SHADING AVOIDANCE FOR A PHOTOVOLTAIC (PV) FARM

(Date received: 14.02.22/Date accepted: 16.03.23)

Thum Peng Chew[1], Sean Lee Xi Xian[2*]

[1]TPC Solutions, No. 3 Jalan SS24/19, 47301 Petaling Jaya, Kuala Lumpur, Malaysia

[2]Jacobs Engineering Group Malaysia Sdn Bhd,
Suite E-17-P2, Level 17 (Penthouse), Block E, Plaza, No. 2, Jalan Kiara, Mont Kiara,
50480 Kuala Lumpur, Malaysia

[*]Corresponding author: xixianlee@hotmail.com

ABSTRACT

The special requirement of a PV farm lightning shielding system is that it should not introduce shadow on the active PV surfaces so as to avoid impaired PV generation output. By using a simple, repeatable-unit PV row made up of single or multiple PV strings, the problem of finding a cost-effective and efficient PV row lightning finial arrangement can be resolved. The shading analysis combined with the MS IEC 62305 implementation of the Rolling Sphere Method (RSM) is able to give a simple procedure that lends itself to spreadsheet calculations pertaining to PV farm lightning shielding design.

Keywords: Core Shadow, Lightning Air Termination, Shading Avoidance

1.0 INTRODUCTION

Unlike traditional lightning protection approaches, the special requirement of a PV farm lightning shielding system is that it should not introduce shadow on active PV surfaces so as to avoid impaired PV generation output. While sophisticated software programs are now available for the analysis of air termination systems, what is lacking is for shading analysis to be built into the same program to handle the PV shading problem concurrently. A PV farm is built-up of many PV rows. By using a simple, repeatable-unit PV row made up of single or multiple PV strings, the problem of finding a cost-effective and efficient PV row air termination system is simplified.

The purpose of this paper is to present a simplified and robust method of determining lightning finial arrangement on a PV row taking into account the shading effect that is introduced by its finial core shadow (umbra) at certain times of the day. First, it addresses the core shadow formation then does the shadow analysis to determine inter-row separation for shading avoidance. With inter-row separation and row pitch (inter-row spacing) determined, it proceeds with the RSM to determine the finial length and finial spacing on the PV row. Because the whole analysis could be done on a unit PV row basis, it lends itself to be repeated over the PV farm. Its simplicity also lends itself to spreadsheet implementation.

2.0 STRUCTURE OF THE PV FARM

The PV farm structure is characterised by an extensive low-height and isolated-surface area. It physically resembles a shielded open-structure since the PV module perimeters are made of aluminium frames that are bonded and earthed in each string/row arrangement. Most stroke terminations are characterized by overhead downward flashes with little or no side stroke terminations because of the PV row's low height. There are generally, 2 ways of providing lightning shielding. The first is by adding external steel finials to the natural component LPS. The second makes use of the available PV module aluminium frames as natural air termination in an effort to save cost. Cost-saving considerations also compel the natural components of the PV module support structure and foundations to be used as the LPS down-conductor system and earthing system as shown in Figure 1.

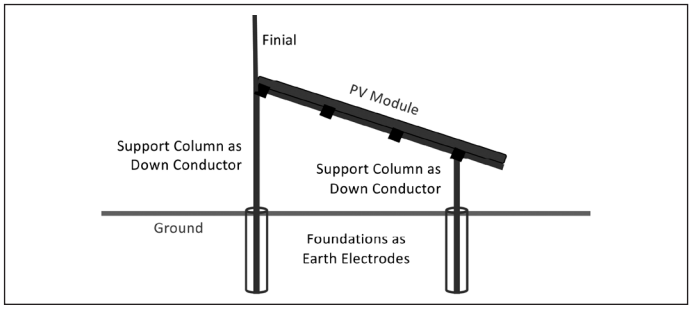

Figure 1: PV Module Support Structure Acting as LPS

In most cases, the aluminium frames are not inherently designed or intended as air terminations. They do get damaged by hotspot punctures at the point of stroke attachment. A more satisfactory engineering solution may be achieved by adding to the natural-component LPS, steel finials arranged on the ridge of

the inclined PV row [1]. Their role is to preferentially intercept lightning strokes while the aluminium mesh's role is relegated to the screening and current distribution functions. With such a method, the PV string shielding failure is determined by finial height and finial positioning/spacing.

3.0 SHADING FROM AIR TERMINATIONS

If air terminations are provided for lightning protection, they may present dynamic shading impacts to the active PV surfaces on which their shadows fall [2]. Dynamic shading possibility depends on the core shadow (umbra) length formed by opaque above-PV-surface objects in accordance to the sun's elevation and direction. The space beyond the core shadow exhibits a diffuse shadow from its penumbra which presents less impact on PV module output. Thus, air termination must be placed such that their core shadows do not fall on active PV surfaces. There are 2 types of air terminations, namely the tall mast and the short finials. The following section evaluates their possible applications in the PV farm.

3.1 Core Shadow Formation with the Umbra

In practical situations, only umbra shadows are assumed to have significant shading impacts on PV surfaces. In contrast, penumbras produce weak shading intensities. A simple shadow analysis is made here to determine the core shadow transitions of narrow/thin to wide vertical objects. In general, umbra shadow formation depends on 3 factors, namely :-

1. The length of the object's umbra is taken to be proportional to its width, e.g. for a finial of diameter, d_f, , its umbra length, L_u formed in space is fixed at 108 x d_f as shown in Figure 2a. The constant is the ratio of the sun's distance from Earth and the sun's diameter [3, 4].
2. The sun's elevation angle, α above the horizon determines the umbra's inclination.
3. The height, H of the object above the ground to produce an inclined umbra layer and surrounded by its penumbra in space; the thickness of the umbra above the ground is determined by the object's height. A shadow is formed on the ground if this inclined but length- and thickness-limited umbra layer intersects the ground.

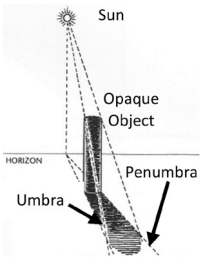

Figure 2a: Vertical Rod's Umbra and Penumbra Illustrated

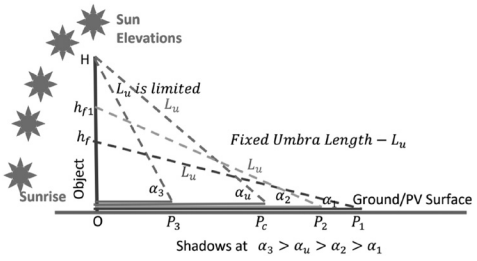

Figure 2b: Shadow Formation with Vertical Object

Figure 2b illustrates how shadow is formed as the sun rises. When the sun's elevation angle, α is zero, there is no umbra intersection with the ground because the umbra volume lies just above the ground plane and no shadow is formed. As the sun rises low in the horizon, the full umbra length, L_u initially forms the shadow at a small elevation angle, α_1. While the umbra's lower region intersects the ground plane at full umbra length, L_u, its upper volume still lies in the space above the ground. It contributes partially to the shadow OP_1 on the ground. The shading intensity is weak. As the sun rises, α increases to α_2. The umbra length, L_u inclines and forms its shadow, OP_2 on the ground as shown in Figure 2b. Its intensity increases. In general, the shadow length,

$$L_s = L_u.\cos\alpha \qquad \text{where } \alpha < \alpha_u \tag{1}$$

This continues until the shadow length is OP_c at sun elevation angle α_u. This critical angle defines the height on the object ($h_f = H$) that produces the full umbra length, L_u just touching the ground. At greater heights, the umbra length produced is too short to touch the ground. Thus, angle, $\alpha_u = sin^{-1}\left(\frac{H}{L_u}\right)$ and the shadow geometry makes a transition at $H = L_u$.

When the sun rises beyond this elevation angle at say, $\alpha_3 > \alpha_u$, the ground-intersecting umbras are formed by the object's surface at heights less than H. The shadow length, OP_3 is hence, fixed by H. The shading intensity is high but the shadow length, L_s is given by :-

$$L_s = H/\tan\alpha \qquad \text{where } \alpha \geq \alpha_u \tag{2}$$

If the width of an object is 1 metre, L_u will be 108m. If the object's physical height is shorter, then its umbra-limit angle, α_u is small. Its L_u- transition will occur a short while after sunrise with a long shadow. In contrast, a thin blunt-tipped finial with short umbra length will have its umbra-limited angle, α_u at 90°; its shadow is umbra-length limited with no transition.

3.2 Shadow Analysis

Table 1 shows the calculated shadow lengths on the ground surface of a tall mast and of a short blunt-tipped finial. Within the practical range of finial diameters (8mm to 16mm), the umbra length ranges from 0.86m to 1.73m. A 14 mm diameter finial is selected for comparison with a typical 150mm diameter lightning mast of height 6.5m. The umbra-limited angle, α_u for both air terminations exceeds 20°. Equation (1) is appropriate to be used in the just-after-sunrise shading analysis. But compared with the finial, the mast length transits to Equation (2) after 23.66°.

For any PV farm location, the time of allowable umbra shading has to be limited to the early hours of the morning and late hours of the evening. This time should be specified so that an object's core shadow does not produce adverse impact on PV generation output. In practice, it could lie between 7.30am and 8.30am such that the finial's shadow cast by the sun is short and it will not fall on any active PV surface at times later.

Table 1 shows that the mast's shadow length on the ground is much longer than that of the finial. At a sun elevation angle of 30°, a 6.5m lightning mast requires a shading clearance of 11.258m on the ground as compared to 1.309m for a short finial. The shorter finial shading clearance may be allowed to fall in the PV inter-row separation space. Thus, shading impact is easier to mitigate with the multiple finial solution than the single tall-mast solution. The former resolves the problem at the PV row level while the latter needs 8.6 times larger shading clearance on the PV farm ground.

Table 1: Comparison of Mast and Finial Shadow Lengths

	Mast	Finial
Height, m	6.50	2.50
Diameter, mm	150.0	14.0
Fixed Umbra Length, m	16.200	1.512
Umbra-Limited Angle, °	23.66	90.00
Sun's Elevation, °	**Shadow Length, m**	
	Mast	**Finial**
5.0	16.138	1.506
10.0	15.954	1.489
20.0	15.223	1.421
30.0	11.258	1.309
45.0	6.500	1.069
60.0	3.753	0.756
80.0	1.146	0.263

4.0 SHADING AVOIDANCE OF FINIALS MOUNTED ON PV ROWS

If multiple finials are opted for lightning shielding at the PV row level, their effectiveness is determined by their vertical length and the spacing between them. Usually, one or more inclined PV strings are grouped to form a PV row. The finials are mounted along the row's ridge (as shown in Figures 1 and 5) and at the high corners. Apart from other considerations, the rows should be orientated such that finial shadows do not fall on neighbouring rows.

4.1 Sun Direction and PV Row Orientation

The formation of shadows depends on the sun's position in the sky and the time-of-day. Its position is defined by its elevation angle, α and its azimuth, Ψ as shown in Figure 3a. The sun's elevation determines an object's projected shadow length while its azimuth determines the shadow's direction relative to a PV row's orientation azimuth; both azimuths by convention are referenced to the North. The sun's azimuth angle may be calculated from either [5] or [6].

The sun's positions in the sky over one full year can be represented in a 2-D Cartesian chart for a specific location on the Earth's surface. Figure 3b shows the sun's path at location P Latitude 3.1°(north of the Equator), Longitude 101°(in Peninsular Malaysia). It can be used to orientate the PV row to avoid shading as well as to optimise generation output. Based on Figure 3b, PV operation considerations may adopt a 30° sun's elevation corresponding to 8.00am and a 120° azimuth angle, A.

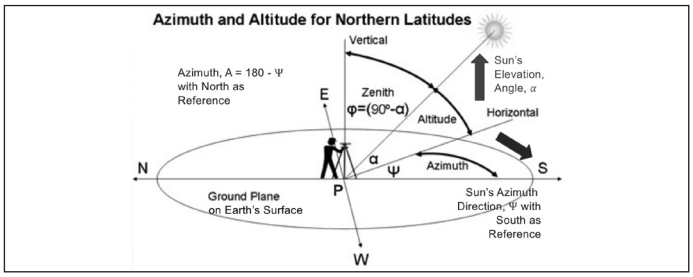

Figure 3a: The Sun's Angles with Reference to Northern Latitudes

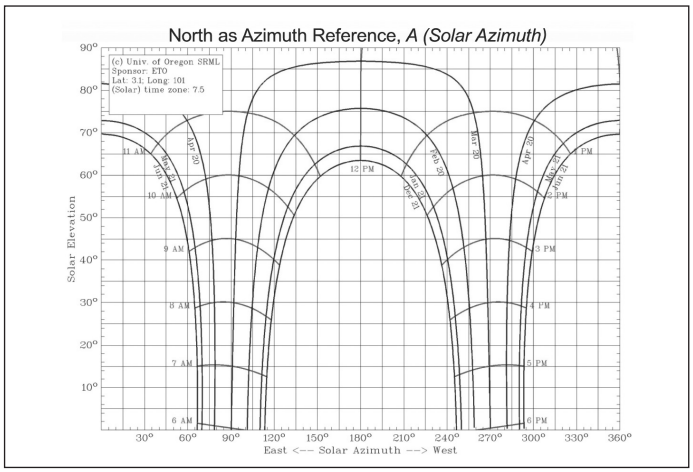

Figure 3b:University of Oregon 2-D Sun Path Chart for Latitude 3.1° and Longitude 101° [7]

4.2 Shadow Length and Shading Avoidance

For low shading impact, a finial has to be short and thin. It's length is determined from shading analysis and its diameter must satisfy Table 6 requirements of MS IEC 62305-3 [8].

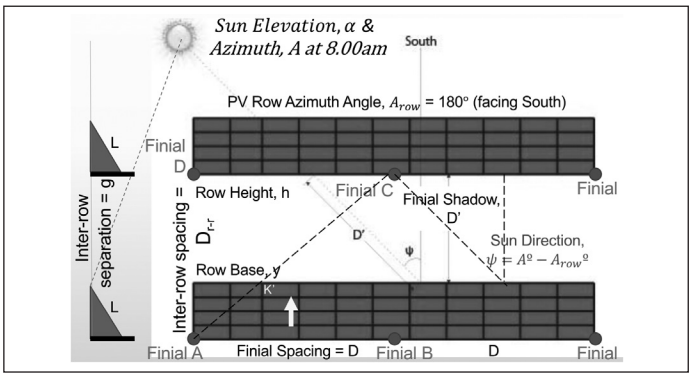

Figure 4: Plan View - Sun Direction and PV Row Orientation

Figure 4 is used to obtain the PV inter-row separation, g. Table 1 gives the umbra length, L_u = 1.512m. For the sun elevation angle, α = 30°, the shadow length, L_s = D' = L_u.cos 30° = 1.309m.

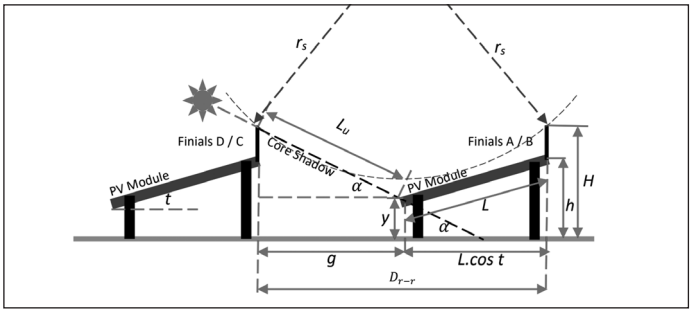

Figure 5: D_{r-r} Elevation View of 2 PV Rows with Finials Showing Row Pitch and Rolling Sphere

The PV row is usually orientated facing South-east to South at azimuth angle, A_{row} between 150° and 180°. The South-east orientation angle (150°) gives a larger shadow length. ψ as shown in Figure 3a, is given by

$$\psi = A - A_{row} \quad (3)$$
$$= 120° - 150°$$
$$= -30°$$

From Figures 4 and 5, the PV inter-row separation, g, is given by

$$g = D'.\cos\psi = 1.309\ \cos(-30°) = 1.134\text{m} \quad (4)$$

Thus, to avoid shading for a PV row orientated in the 150° (south-east) direction, the inter-row separation must be at least 1.134m. If the row is orientated to face the sun at which $\psi = 0°$, the inter-row separation for 8.00am at location P is then 1.309m. The PV inter-row separation is normally used as an access way for construction, operation and maintenance. As such, g has a minimum width which generally is 1.0m. In this case, g is larger than 1.0m, hence shading avoidance take precedence with g increased to 1.134m.

For a given row's inclined width, L on the PV module surface and tilted at an angle of t°, the row spacing or pitch, $D_{r\text{-}r}$ as shown in Figures 4 and 5, is given by

$$D_{r\text{-}r} = g + L.\cos t \quad (5)$$

Hence, if L is 4m and the PV row's tilt angle is 10°, the row pitch, $D_{r\text{-}r}$ is 5.073m.

5.0 LIGHTNING RSM SHIELDING ANALYSIS

The purpose of lightning shielding is to position equal-height finials on the PV row's ridge in relation to neighbouring PV rows so that they prevent direct lightning strikes to the PV modules. The MS IEC 62305 rolling sphere method [9] is employed in the analysis to find the finial length, L_f and finial spacing, D such that a group of finials can prevent a rolling sphere from coming into contact with the inclined PV module surface.

The relevant shielding geometry is depicted in Figure 4 with 4 finials placed at the corners of a rectangular block having ground length, D and ground width, $D_{r\text{-}r}$. The length of the diagonal on the ground plane is $D_d = \sqrt{D^2 + D_{r-r}^2}$. D_d is depicted along the block's A-C section view in Figure 6. The rolling sphere radius, rs is calculated from the minimum interception stroke current, I in kA based on the desired probability of shielding. It is given in MS IEC 62305 [9] as

$$r_s = 10I^{0.65} \quad (6)$$

Based on a given design interception current, the penetration depth, p of the greater circle of the rolling sphere into the block ABCD is as follows:-

$$p = r_s - \sqrt{r_s^2 - 0.25D_d^2} = r_s - \sqrt{r_s^2 - 0.25(D^2 + D_{r-r}^2)} \quad (7)$$

For real application of the expression, D_d has to be limited by the condition: $0.5D_d < r_s$.

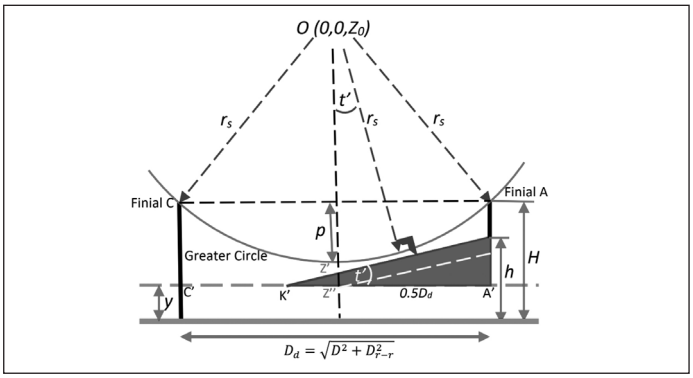

Figure 6: A-C-C'-A' (D_d) Vertical Plane Containing Rolling Sphere

5.1 Finial Length Analysis for Sphere Rolling Over the PV Row's Ridge

By substituting D_d with D into the p expression, the finial length, L_f on the D-section of the block containing the PV row's horizontal ridge can be evaluated by $r_s - \sqrt{r_s^2 - 0.25D^2}$.

For inclined surfaces of the block, their required finial lengths are derived in the Appendix.

6.0 DIMENSIONS OF FINIAL SYSTEM

Figure 7 illustrates the manner in which the finial length and spacing are determined for a representative 30m long PV row in Malaysia. Typically in Malaysia, the tilt angle, α of the PV row is around 10°. The PV row may at the extreme, face South-east (ψ=-30) for which the inter-row separation, g is taken to be 1.309m. For a PV inclined surface width, L of 4m, a row pitch, $D_{r\text{-}r}$ of 5.073m is required. The height of the PV row's ridge, h-y is 0.695 m. Along the PV row's ridge, a number of finials can be provided depending on the cost and the desired interception efficiency of the finial system.

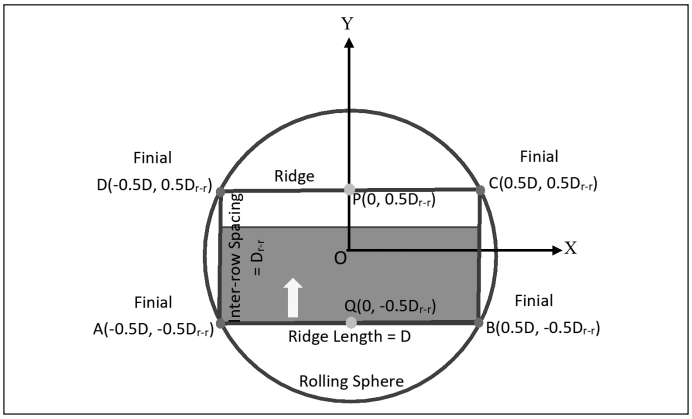

Figure 7: Plan View of Rectangular Block ABCD with Rolling Sphere

For inclined surfaces, the rolling sphere is shown in Figure 7. The finial length calculations are implemented in a spreadsheet. Table 2 summarises the finial length results from the analysis of various row sections for various finial spacings. The PV row's ridge requires the longest finial length because it presents the largest lightning exposure whereas the D_d and the $D_{r\text{-}r}$ planes are generally less exposed due to the row's inclination. Thus, it seems that in this case, the finial length of a PV row is determined by its ridge.

Table 2: Finial Lengths for Various Finial Spacings With PV Row Orientated at 150° Azimuth

PV Row Length, m	30.00	Finial Length, m			
No. of Equal Finial Sections per Row	Finial Spacing, D m	$D_{r\text{-}r}$ Plane	D_d Plane	Row's Ridge	PV Row
1	30.000	0.000	6.358	6.563	6.563
2	15.000	0.000	1.182	1.427	1.427
3	10.000	0.000	0.402	0.621	0.621
4	7.500	0.000	0.160	0.347	0.347

Table 2 also shows that the minimum finial length required varies quite substantially with finial spacing. If a row is a single section, the finial length at the ends of the row will have to exceed 6.563m; a height equivalent to that of a single tall mast. As deduced from Table 1, it does not have a shading clearance advantage. Neither does it have a land-use and cost advantage. Design and construction considerations favour the multi-section options of either 2, 3 or 4 equal sections per row. The final selection depends on design optimisation and cost.

Since the PV row's ridge will attract a large number of lightning terminations, it is necessary to examine the impact of shorter finial lengths on the ridge's lightning exposure whose expression is derived in the Appendix. Table 3 shows that reduction in length incurs larger ridge exposures. Hence, finial lengths must always be adequately provided.

Table 3: Impact of Compromised Finial Length on PV Row's Ridge Lightning Exposure

Finial Spacing, D m	**15.0**	**10.0**	**7.5**
Row Finial Length, L_f m	1.427	0.621	0.347
Dd Finial Length, l m	1.182	0.402	0.160
% Finial Short, 100(1-l/L_f)	17.14	35.28	53.84
Ridge Exposure, D_e m	6.303	5.969	5.514
% Exposure, 100. D_e/D	42.02	59.69	73.52

Table 4 compares the finial lengths on the basis of finial spacing, PV row orientation and interception current. For a given interception current, the finial length does not change with PV row orientation azimuth. This consistency confirms that lightning exposure is independent of row orientation.

Table 4: Finial Length Comparison for Two PV Row Orientations and Three Interception Currents

Interception Current/ Probability*/ Striking Distance	3 kA / 99.0% / 20.42m		2.5 kA /99.2% / 18.14m		2 kA / 99.5%/ 15.69m	
Azimuth, °	150	180	150	180	150	180
No. of Sections/ (Finial Spacing)	**Min. Finial Length, m**		**Min. Finial Length, m**		**Min. Finial Length, m**	
2 /(15m)	1.427	1.427	1.623	1.623	1.908	1.908
3 /(10m)	0.621	0.621	0.703	0.703	0.818	0.818
4/(7.5m)	0.347	0.347	0.392	0.392	0.455	0.455

Note: * - Probability of the interception current being exceeded.

It is noted that a 15m section requires a taller finial, (greater than 1m) compared to a 10m section. If the finial length is to be less than 1m, the suitable finial spacings are between 7.5m to 10m. In this range, the finial mounting and connection to their support structure as shown in Figure 1, may have to be evaluated with costs for the selection of finial spacing and length.

A more significant change in finial length comes from the change in the interception current. A lower design interception current with higher exceedance probability will achieve a higher finial interception efficiency because the greater stroke currents would not penetrate the shielding system. While MS IEC 62305-1 [9] suggests a 99% efficiency with a 3 kA design current for LPL I, a 2 kA design current can give 99.5% interception efficiency. In terms of overall performance, construction and quantity of materials used, the 2 shorter sections only require standard finial lengths in the range of 0.5m to 1.0m which is less than L_u (= 1.512m from Table 1) to achieve the required interception efficiency as suggested in [1].

7.0 CONCLUSION

Shadow formation analysis suggests that between a short finial and a tall mast, shading avoidance in a PV farm is better achieved with multiple short finials than single tall masts. The former resolves the problem at the PV string/row level while the latter needs a larger surrounding shading clearance area. In order for finials not to create significant shading impact, the pitch between PV rows must be sufficient so that the finial's core shadow will not encroach into the neighbouring rows. This core shadow length is a function of the sun's elevation and azimuth and the row's orientation and tilt angle. It is shorter than that of a tall mast and may be designed to fall within the inter-row separation space.

The expression for the height and length of a finial with respect to inter-finial spacing for an inclined PV row surface is derived using the RSM. Investigation with the range of finial lengths is made with inter-finial spacings that are likely to be encountered in practice. The finial design procedure also examines the impact on PV row's ridge lightning exposure as a result of shorter finial lengths. It concludes that finial lengths must always be adequately provided. Technical comparison points to simple short finials of 0.5m to 1.0m in length which is less than its umbra length. It leads to the prospect of a multi-section design for a 30m PV row. For cost-effectiveness in practice, the PV row may be divided into 2, 3 or 4 equal sections. A simple approach for the implementation of lightning shielding system with shading avoidance for a PV farm is demonstrated. Its calculation can be easily made with a spreadsheet. ■

APPENDIX - DETERMINING FINIAL LENGTHS

A.1 The Coordinate of the Centre of the Rolling Sphere, O(0, 0, Z0)

In order to prevent the circle in Figure 6 from touching the inclined PV module surface, the finials' minimum protruded length for a given PV row height, h and a tilt angle, t is determined geometrically. The height of the PV row's ridge is

$$h\text{-}y = L.\sin t \quad \text{(A1)}$$

Applying the Similar Right Angle Triangle Theorem to the ratio of sides in Figures 4 and 6,

$$\frac{A'K'}{L.\cos t} = \frac{D_d}{D_{r-r}} \text{ giving } A'K' = \frac{D_d}{D_{r-r}}.L.\cos t \quad \text{(A2)}$$

and from Figure 6, the diagonal tilt angle, t' is given by

$$tan\ t' = \frac{h-y}{A'K'} = \frac{(h-y).D_{r-r}}{D_d.L.\cos t} = \frac{D_{r-r}}{D_d} tan\ t \quad (A3)$$

$$\text{and } \sec t' = \sqrt{1 + \left(\frac{D_{r-r}}{D_d}\right)^2 tan^2 t} \quad (A4)$$

The angle t' reaches a physical maximum when the rolling sphere circle touches the PV row's ridge. Its maximum is given by

$$sin\ t'_{max} = \frac{D_d}{2r_s}$$
$$\text{or } t'_{max} = sin^{-1}\left(\frac{D_d}{2r_s}\right) \quad (A5)$$

Beyond it, the sphere rolls over the PV row's ridge. Thus, the analysis of Figure 6 A-C plane is made with $t' < t'_{max}$.

The diagonal plane A-C-C'-A' in Figure 6 is treated as an X-Z plane. Applying coordinate geometry to the plane, the gradient and intersect of the inclined PV surface line are :-

Line's gradient = $tan\ t'$

Its fixed intersect at X = 0 with the Z-axis, $Z'Z'' = (h\text{-}y) - 0.5D_d.tan\ t' = (h\text{-}y) - 0.5D_{r\text{-}r}.tan\ t$

$$\text{The vertical length } OZ' = r_s.sec\ t' = r_s \sqrt{1 + \left(\frac{D_{r-r}}{D_d}\right)^2 tan^2 t} \quad (A6)$$

Thus, the Z-coordinate of centre, O of the rolling sphere is :-

$$Z_0 = OZ' + Z'Z'' = r_s \sqrt{1 + \left(\frac{D_{r-r}}{D_d}\right)^2 tan^2 t} + (h\text{-}y) - 0.5D_{r\text{-}r}.tan\ t \quad (A7)$$

A.2 Sphere Sitting on top of the Block ABCD

The equation of the rolling sphere whose plan view is depicted in Figure 7, is

$$(Z - Z_0)^2 + Y^2 + X^2 = r_s^2$$

$$Z = H - y = Z_0 \pm \sqrt{r_s^2 - X^2 - Y^2} \quad (A8)$$

The RSM is being applied to the ABCD rectangular section which has its mid-point below the rolling sphere's centre O and its corners A, B, C and D. For $H\text{-}y < Z_0$ and $0 \le t' < t'_{max}$,

$$H - h = r_s \sqrt{1 + \left(\frac{D_{r-r}}{D_d}\right)^2 tan^2 t} - 0.5D_{r\text{-}r}.tan\ t - \sqrt{r_s^2 - X^2 - Y^2} \quad (A9)$$

Thus, for a given a striking distance, the finial length depends on the finial spacing, the PV row pitch and its tilt angle.

For example, if the coordinate of the finial at corner A is (-0.5D, -0.5$D_{r\text{-}r}$, H-y), finial A's length,

$$L_f = H - h = r_s \sqrt{1 + \left(\frac{D_{r-r}}{D_d}\right)^2 tan^2 t} - 0.5D_{r\text{-}r}.tan\ t - \sqrt{r_s^2 - 0.25D^2 - 0.25D_{r-r}^2}\ .$$

Symmetry ensures the 3 other corners B, C and D have the same finial length as A.

In the case of $t' \ge t'_{max}$, $L_f = 0$ implying that the PV row's ridge is a natural air termination. However, for reasons given in [1], the PV module's thin aluminium frame should not be used. Hence, the need for extraneous finials on the ridge at corners A, B, C and D.

A.3 Sphere Rolling along the Ridges of Planes AB and CD from BC to AD

Based on Figure 5, the finial length can also be evaluated for the $D_{r\text{-}r}$ section in which case,

$$L_f = r_s.sec\ t - 0.5D_{r\text{-}r}.tan\ t - \sqrt{r_s^2 - 0.25D_{r-r}^2} \quad (A10)$$

which is valid for $0 \le t < t_{max}$. Similarly, in the case of $t \ge t_{max} = sin^{-1}\left(\frac{D_{r-r}}{2r_s}\right)$, $L_f = 0$. Lightning shielding is naturally provided by the PV row's ridge at corners A, B, C and D.

A.4 Sphere Rolling Over PV Row's Ridges of Planes AB and CD

In the vertical planes AB and CD that contain the finial spacing D, the finial length, L_f is determined from its sphere rolling over the ridge with penetration depth given by

$$p = L_f = r_s - \sqrt{r_s^2 - 0.25D^2} \quad (A11)$$

A.5 Ridge Exposure due to Shortened Finial Length

Being the highest line on the PV row, the ridge has a higher probability of stroke attachment. If the finial length is compromised with $l_f (< L_f)$, then the rolling sphere surface will intersect the ridge and expose it to lightning attachments. By RSM according to [8], the exposure length is

$$D_e = 2\sqrt{r_s^2 - (r_s - l_f)^2} \quad (A12)$$

REFERENCES

[1] Thum Peng Chew and Sean Lee Xi Xian, 'The Impact of Direct Lightning Strike Damages on PV Modules In a Large Malaysian PV Farm', published in IEM Journal Vol. 82, No. 2, December 2021.

[2] Peter Bulanyi and Rodd Zhang, 'Shading Analysis & Improvement for Distributed Residential Grid-Connected Photovoltaics Systems', The 52nd Annual Conference of the Australian Solar Council, Solar 2014.

[3] Sun Fact Sheet - http://nssdc.gsfc.nasa.gov/planetary/factsheet/sunfact.html.

[4] Sun - https://en.wikipedia.org/wiki/Sun.

[5] Solar Azimuth Angle - https://en.wikipedia.org/wiki/Solar_azimuth_angle.

[6] Taiping Zhang, Paul W. Stackhouse Jr., Bradley MacPherson and Colleen Mikovitz, 'A Solar Azimuth Formula that Renders Circumstantial Treatment Unnecessary Without Compromising Mathematical Rigor: Mathematical Setup, Application and Extension of a Formula Based on the Subsolar Point and Atan2 Function', Renewable Energy Vol. 172, pp 1333-1340, 2021.

[7] http://solardat.uoregon.edu/SunChartProgram.html.

[8] MS IEC 62035 - Protection Against Lightning - Part 3: Physical Damage to Structures and Life Hazard, 2010.

[9] MS IEC 62035 - Protection Against Lightning - Part 1: General Principles, 2010.

PROFILES

THUM PENG CHEW graduated with the B. E. and the M. Eng. Sc. degrees from the University of Malaya. He is a Professional Engineer and a Fellow of IEM. He was a consultant specialised in electric power systems, lightning protection and earthing. He still has continuing interests in these areas.
Email address: thumpc@gmail.com

SEAN LEE XI XIAN graduated with Bachelor of Electrical Engineering (Hons) from Multimedia University, Malaysia. He is a Professional Engineer registered with Board of Engineers Malaysia, Professional Technologist registered with Board of Technologist, Grid Connected PV (GCPV) Qualified Person registered with SEDA, Corporate Member of IEM and ASEAN Chartered Professional Engineer. He has extensive experience in substation primary detailed design and multi-disciplinary interfacing for MV, HV and EHV substation (up to 500kV). Apart from substation engineering work, he is also involved in renewable energy sector and energy storage system projects.
Email address: xixianlee@hotmail.com

TREND STUDY ON COVID-19 PANDEMIC LOCKDOWN IMPACT ON RIVERS IN SELANGOR, MALAYSIA

(Date received: 31.08.2022/Date accepted: 07.04.2023)

Aini Hidayati Shahrir[1,2], Gasim Hayder[1,3*]

[1]Department of Civil Engineering, College of Engineering, Universiti Tenaga Nasional (UNITEN), 43000 Kajang, Selangor Darul Ehsan, Malaysia

[2]School of Civil, Environmental & Mining Engineering, The University of Adelaide, SA 5005, Australia

[3]Institute of Energy Infrastructure (IEI), Universiti Tenaga Nasional (UNITEN), Kajang 43000, Selangor Darul Ehsan, Malaysia

[*]Corresponding author: gasim@uniten.edu.my[1,3]

ABSTRACT

According to the Department of Environment, numerous rivers, and streams in Selangor, and practically all rivers, are in the 'polluted' and 'slightly polluted' category even before the COVID-19 outbreak. Due to a lack of anthropogenic activities such as industrial discharge, agricultural, poultry, sediment, and silt erosion, the trend of pandemic lockdown on water quality parameters in Selangor is expected to decline. The goal of this research is to see if contamination of water resources and rivers increases or decreases during a pandemic by examining the trajectory of water quality parameters in relation to the COVID-19 pandemic, to figure out which parameters are affecting pollution in Selangor rivers, and to emphasize the water quality in each river for Department of Environment, utilizing data from 2016 to 2020. The results of the investigation revealed significant variations in water and wastewater quality over time as it shows anthropogenic activities decrease during pre-pandemic and pandemic lockdown periods. DO, TSS, ammoniacal nitrogen, and turbidity exhibited decreasing value on most water quality metrics except for BOD, COD, and pH levels during the lockdown period.

Keywords: COVID-19, Lockdown Period, Malaysia, Pandemic, Selangor, Water Quality

1.0 INTRODUCTION

The COVID-19 pandemic has taken the world by storm and caused unpredictable damaged towards all aspect including water resource in Malaysia. The management of water resource reflects the development of water quantity and quality in Selangor. The tendency for the water resource and their demands in Malaysia to rise was estimated to be 60% in 2010 and 113% in 2020 forecasted in 1995 [14].

The classification of water quality in Malaysia is reference to DOE and the contributing factors are determined with the comparison of water quality parameters [1]. Studying the water quality of rivers can identify the main source of pollution of the river such as anthropogenic, lithological, atmospheric, or climatic [2]. Polluted rivers caused toxic and disruption to the endocrine system of aquatic life [31].

It can be summarized that the source of contamination is mainly due anthropogenic activities which originated from industrial, agriculture, poultry, farming and soil erosion [14], [17]. There are much evidence of pollution and contamination in rivers in Selangor, one evidence can be seen that Klang River has heavy metal contamination in their water bodies[32]. It was found that Semenyih river in Selangor are highly polluted with PO_4 and faecal coliform [17]. The degradation of water quality in Selangor was associated with algal blooming and eutrophication especially in Selangor River [14].

The trend of COVID-19 pandemic lockdown towards the water quality in River in Selangor is predicted to decrease due to lack of anthropogenic activities mainly from industrial discharge, agriculture, poultry, sediment, and silt erosion. The study gap focused on pollution in most rivers in Selangor has been steadily expanding over the previous decade [13], raising the question of whether contamination in water resources and rivers increases or decreases during pandemics.

As there are lack of study in water quality parameter effects by the pandemic lockdown, this suffices the need for more research in this area. This research has societal benefits such as the study of water quality before and during the COVID-19 pandemic, the impact of the COVID-19 pandemic on the water and wastewater sector, changes in water pollution before and during the COVID-19 pandemic, recommendations for future rejuvenation strategies if needed, awareness of the importance of water quality in society, and justification of water quality importance. According to [21], only water and air quality have been examined as environmental implications for the lockdown period. The investigation of the influence of COVID-19 is still regarded innovative and a viable research platform. This study contributes the need of further rejuvenation and mitigation actions to increase the water quality classes for the rivers in Selangor to ensure there will availability of safe and clean water

resources for future use.

Despite being Malaysia's most developed state, Selangor continues to be one of the most affected states when it comes to water shortages. Selangor has been identified as the state with the most water supply concerns, with 49.5 percent in 2016 and 62.4 percent in 2017 [6]. With the pandemic in full swing, a scarcity of water means a lack of cleanliness, which increases the danger of virus transmission. In recent years, Malaysia's water resource concerns have risen in scope and complexity. This is due to the fact that Malaysia has converted a large portion of its land from agriculture to urban–industrial–commercial use [31].

The study focuses on the impact of COVID-19 pandemic period towards the water quality and wastewater in Selangor district only. Given that water contamination is common in Selangor, it has wreaked havoc on the state's water supply. This is a comprehensive study of the physical, chemical, and biological characteristics of both water and wastewater to investigate the differences in water quality before, during, and after the MCO period, which coincided with the global lockdown to stop the spread of SARS-CoV-2 viral transmission of COVID-19 in the state.

The aims of this paper are to study the trend of water quality parameters with the effect of COVID-19 pandemic and to identify which parameter was the most significant contributor to contamination in the rivers in Selangor.

2.0 METHOD

2.1 Description of Study Area

Selangor is located on the West Coast Peninsular Malaysia ranging the total area of 8,104 km^2. Selangor has around 413 rivers according to Selangor Water Management Authority (LUAS). The average annual rainfall is 2236 mm with 88.0 inch per year. The study areas comprised on 19 rivers in Selangor which are Ampang River, Balak River, Buloh River, Chuau River, Damansara River, Gombak River, Guntong River, Keroh River, Klang River, Kundang River, Langat River, Penchala River, Rambai River, Rawang River, Selangor River, Sembah River, Semenyih River, Sepang River, and Serendah River.

2.2 Data Collection and Timeline

The data is collected from the Department of Environment and undergo standard water sampling collection and the period of the data ranges from 2016 until 2020. The timeline for the study was from 2016 to 2020. The data of 2021 was available during the writing of this paper. However, there are certain data of rivers that only provide 2017 to 2020 data. The years 2016-2018 are referred as before pandemic lockdown, 2019 as pre-pandemic lockdown, and 2020 as pandemic lockdown in this study.

2.3 Water Quality Parameters

The water quality parameters studied in this paper consist of Dissolved Oxygen (DO) percentage, Dissolved Oxygen (DO) concentration, Biological Oxygen Demand (BOD) concentration, Chemical Oxygen Demand (COD) concentration, Total Suspended Solids (TSS) concentration, pH value, Ammoniacal Nitrogen (NH_3-N) concentration and turbidity concentration as provided by DOE. These parameters were used to calculate Water Quality Index (WQI) by DOE. WQI has been used in Malaysia for around 28 years and recommended by The Department of Environment Malaysia. It is a collection of water quality recommendations that classify water quality classes based on the quality of water for public use, such as raw water sources, recreational uses, irrigation and aquaculture [24].

3.0 RESULTS & DISCUSSION

3.1 Trend of COVID-19 Lockdown Period and Water Quality Parameters

Figure 1 represents the trend of dissolved oxygen (DO) between the rivers in Selangor. The DO percentage and concentration can be seen decreasing throughout 2016 until 2018 which is before the pandemic period. However, it gradually increased during per-pandemic lockdown and pandemic lockdown period. This is a positive impact as dissolved oxygen is important especially for aquatic lives. If DO is too low, aquatic lives cannot survive as there is not aeration and it leads to higher temperature of water. Since the recent years showed drastic improvements of DO percentage, it can be justified that the COVID-19 lockdown brings significant positive impact towards DO. Nevertheless, the value of average DO throughout the years is still falls underclass I , IIA and IIB for the NWQS (2022) for Malaysia, hence it is still feasible for Malaysian standard for water supply and recreational use.

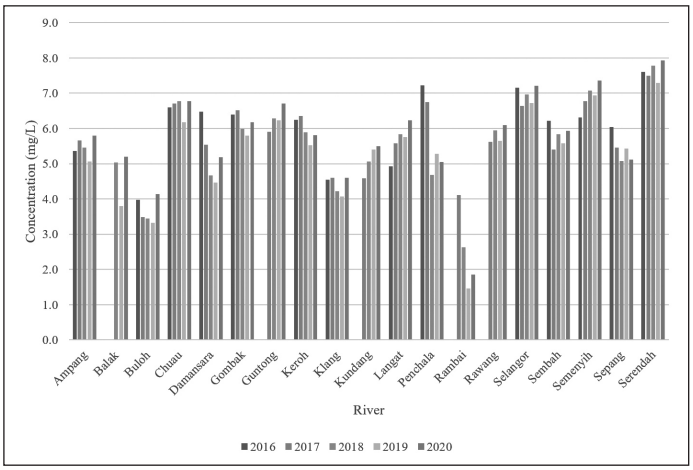

Figure 1: Dissolved Oxygen (DO) Trend

For BOD, there is an uneven trend before the pandemic lockdown period and it gradually increase in pre-pandemic lockdown and during the pandemic lockdown period as shown in Figure 2. This is one of the negative impacts for water quality parameters. Higher BOD is caused by organic pollution and more oxygen is needed for oxygen-demanding species in the water bodies. Thus, it led to lower level of water quality. The increase during the period of lockdown may be due to decaying plants or organic waste that are not treated. Since the majority of water sector are put on hold during the lockdown, this includes the sanitation of water resource to ensure it stayed in it standardised quality. The average BOD falls under the range of class III and IV of NWQS (2022) for water supply but needed extensive treatment and irrigation respectively.

Next, COD concentration gradually increase during the before the pandemic lockdown period but decrease in pre-pandemic lockdown period and increased again during the pandemic lockdown period as illustrated in Figure 3. Similar to BOD, it is considered a negative impact as higher COD means

lower DO in the water bodies. As said previously, DO is crucial for aquatic lives. The COD level relates to the concentration of organic matter in water bodies and it may cause unpleasant smell of the water sources and it contain decaying plants and organic wastes. The COD average falls under the class IIA, IIB and III for NWQS (2022) which is still suitable for water supply and recreational use.

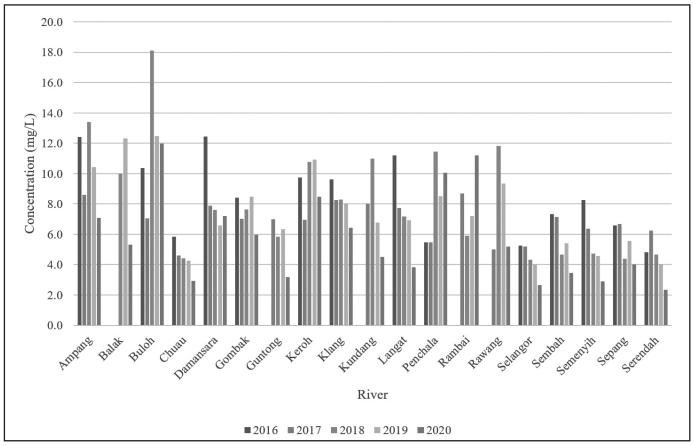

Figure 2: Biochemical Oxygen Demand (BOD) Trend

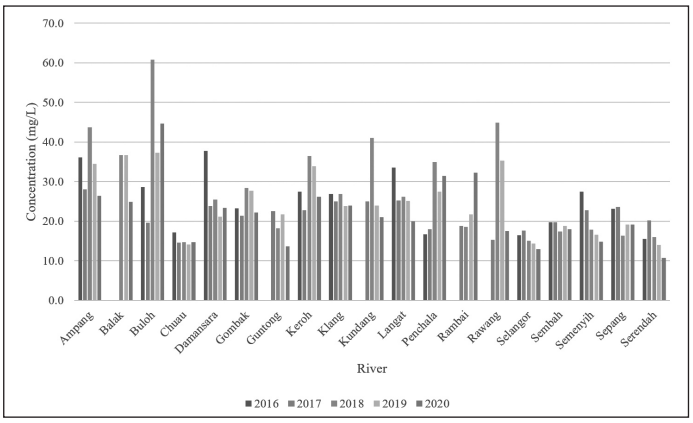

Figure 3: Chemical Oxygen Demand (COD) Trend

Figure 4 exhibits the total suspended solids (TSS) trend, TSS concentration presented an uneven trend during before the pandemic lockdown period but it gradually decreased during pre-pandemic lockdown period and lockdown period. This is a positive impact as lower level of TSS means increase in DO and also help reduced the temperature of water bodies as lesser suspended particles absorbing heat from solar radiation entering the water surfaces. This is a results of lower anthropogenic activities as the it is suspended during lockdown. Lesser particles are discharged and lesser pollution that comes from pesticides, industrial effluent and metals being discharged into the water. The TSS falls under the class I of NWQS (2022) which is suitable for water supply without the need of treatment.

As for the pH value shown in Figure 5, the value remained in a susceptible level as it only experienced minor changes in decimals. The pH level gradually decrease throughout the before the pandemic lockdown, pre-pandemic lockdown period and lockdown period. As pH decrease, hydrogen ion increased and caused the water bodies to become acidic. However, the results of the pH values showed it ranges from the lowest alkaline, neutral and the lowest acid and it falls under class I, IIA, IIB, III, IV which is still under a controlled level of pH value. However, mitigation actions should be put under consideration as the trend seemed to be decreasing throughout the year and it is likely to become more acidic later on.

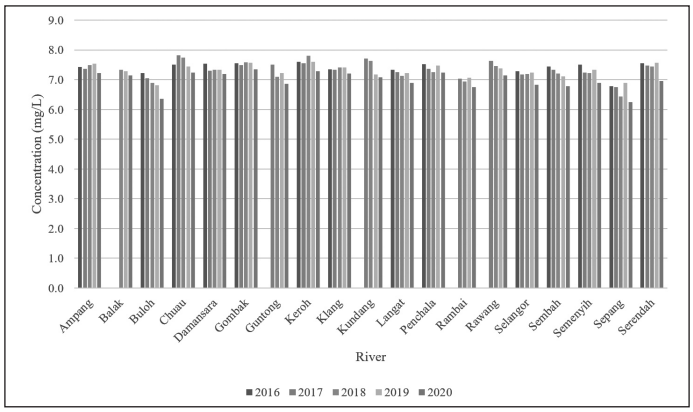

Figure 5: pH Value Trend

The ammoniacal nitrogen trend gradually increased in before the pandemic lockdown and pre-pandemic lockdown period then it decreased during the pandemic lockdown period as presented in Figure 6. Ammoniacal nitrogen is a form of measurement of the level of ammonia in the water bodies. Ammonia typically found in leachate and organic waste. The reduced level of ammoniacal nitrogen is a positive impact of the lockdown. Similar reasons can be concluded as lower anthropogenic activities due to lesser particles are discharged ranging from pesticides, industrial effluent and metals being discharged into the water. Ammoniacal nitrogen falls under the class V of NWQS (2022) which is not suitable for water supply, irrigation and recreational uses. Even though the value is decreasing, further mitigation actions is required to ensure the level of water resources is suitable for use for the coming years.

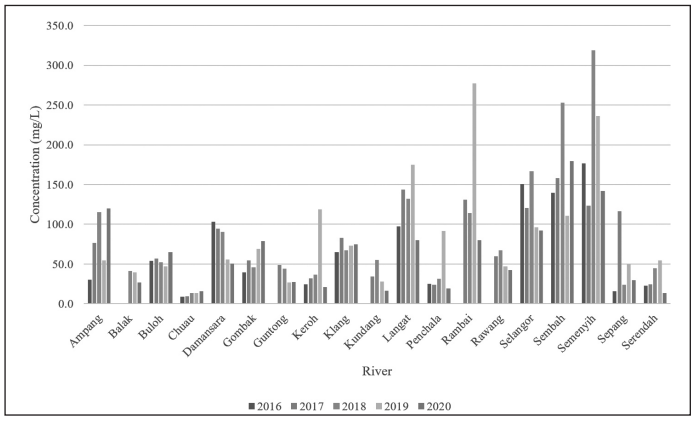

Figure 4: Total Suspended Solids (TSS) Trend

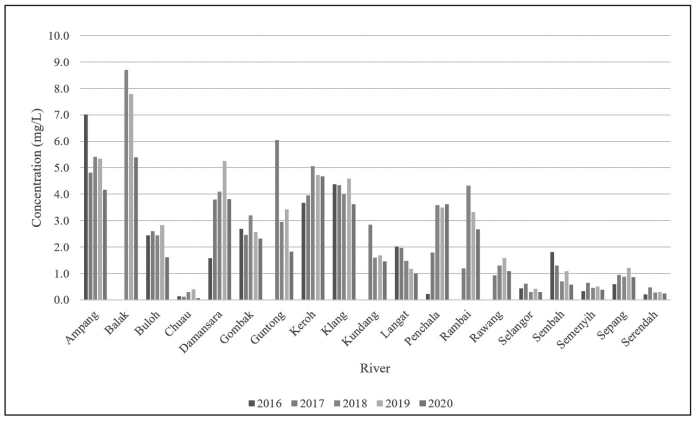

Figure 6: Ammoniacal Nitrogen (NH_3-N) Trend

The average turbidity trend showed uneven trend during before the pandemic lockdown but it then gradually decrease in pre-pandemic lockdown period and lockdown period as shown in Figure 7. Turbidity is affected by DO, TSS, particles and organic matter that are in the water bodies. Lower turbidity level is also a positive impact of lockdown as it signifies lower bacteria, virus and parasites in water bodies. These organisms tend to attached with suspended particles which lead to contamination and pollution of water bodies. This is also the effects of lower anthropogenic activities during the lockdown period. The turbidity however did not fall under any classes of NWQS (2022) hence the level of turbidity is still above the standardised level and further mitigation to reduce the level of turbidity is needed to ensure water resource in Selangor is not polluted.

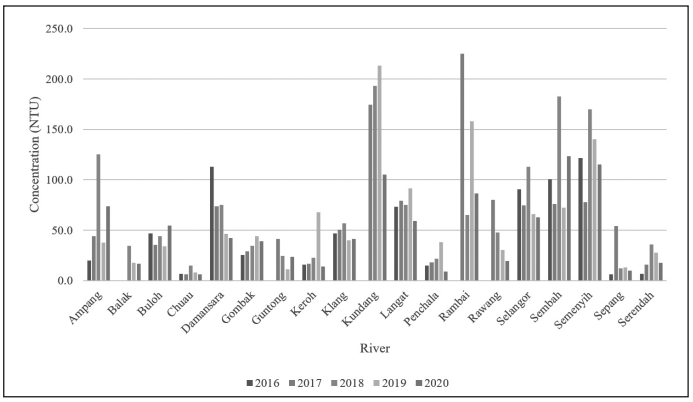

Figure 7: Turbidity Trend

The charts presented had shown significant changes of water and wastewater quality throughout the period. Nevertheless, it is showed positive changes throughout the pre-pandemic and pandemic lockdown period. In water quality parameter perspectives, DO, TSS, ammoniacal nitrogen and turbidity showed positive impacts during the pandemic lockdown period while BOD, COD and pH level have decreased. Even with the positive impact, the turbidity level still above the standardised level of NWQS (2022) and it signifies that the average water resources is still polluted based on the parameter perspective. Mitigation actions is required especially for pH level, ammoniacal nitrogen and turbidity parameter to ensure improved water resources for the coming years. However, there is a possibility for the decreasing value of these parameters may not only be due by anthropogenic activities but also due to external factors that are not studied in this paper.

3.2 The Parameters that Significantly Affected During Pandemic Lockdown

3.2.1 pH Value

Pollution is typically a factor in anthropogenic pH variations. Point source pollution is a frequent cause that, depending on the chemicals involved, can produce an increase or drop in pH. These substances may arise from industrial runoff, sewage discharge, or agricultural runoff. Detergents and soap-based items in wastewater discharge might make a water supply too basic. Typically, the pH of freshwater lakes, ponds, and streams ranges from 6 to 8 depending on the bedrock and soil in the area. The pH of water in deeper lakes where stratification (layering) takes place is often higher near the surface (7.5-8.5) and lower (6.5-7.5) at greater depths.

Temperature differences inside a body of water, where each layer of water does not mix with the layers above or below, are typically the source of stratification. Thermoclines (temperature divides) or chemoclines, which split these layers, exist (chemistry gradients). Oxygen, salinity, or other chemical variables that don't cross the cline, including carbon dioxide, can be the basis for chemoclines. Stratification can result in different pH values along a cline as a result of CO2's impact on water's pH. Due to increasing CO2 from respiration and breakdown below the thermocline, pH values in different water layers differ. The saturated CO2 that has been accumulated in the lake's lower strata is what has caused this huge reduction.

When the pH of water falls below 5.0 or rises above 9.6, harmful repercussions are evident. Due to their adaption to a higher pH, saltwater fish are more susceptible to the negative effects of acidification. Fish are more prone to fungus infections and other physical harm when the pH is below ideal levels. The solubility of calcium carbonate decreases as water pH rises, preventing aquatic creatures from developing shells. At pH values below 5.0, fish reproduction generally suffers, and many species will depart the area. When the pH falls below 4.0, fish start to perish.

Heavy metals may become more soluble at low pH levels. Metal cations including aluminium, lead, copper, and cadmium are released into the water rather than being incorporated into the sediment as the concentration of hydrogen ions rises. The toxicity of heavy metals rises along with their concentration. At levels as low as 0.1-0.3 mg/L, aluminium can inhibit growth and reproduction while raising mortality rates. Additionally, mobile metals can enter organisms during respiration and harm their physiological systems. On the other end of the scale, high pH levels can kill aquatic species at levels over 10.0 by harming their skin and gills. Even at usual concentrations (9.0), ammonia in the water can cause death. Ammonia and water mix to form an ammonium ion at low and neutral pH values.

3.2.2 Ammoniacal Nitrogen

Some types of nitrogen, such as nitrate-nitrogen and ammoniacal nitrogen, can be harmful to aquatic life in very high amounts. Commercial fertilisers and other industrial uses need the production of ammonia. The breakdown of organic waste, gas exchange with the atmosphere, animal and human waste, and nitrogen fixation activities are all examples of natural sources of ammonia. Ammonia can enter the aquatic environment both directly and indirectly. Direct entry points for ammonia include municipal wastewater discharges, animal excretion of nitrogenous waste, and air deposition. The inability of aquatic species to sufficiently expel the toxin when ammonia levels in the water are high enough causes toxic accumulation in internal tissues and blood, which may result in death. Ammonia toxicity to aquatic creatures can be influenced by environmental conditions including pH and temperature.

Ammonia, nitrate, and nitrite are the three major chemical states of nitrogen found in streams. Depending on the dissolved oxygen content of the water, some ammonia contained in river water is transformed to nitrate. As was previously said, nitrate is not particularly hazardous, but if it is present in excess, it begins to transform into nitrite, which is extremely damaging even at low concentrations.

The main cause of the high concentration of ammonium nitrogen in the river was the excessive and ongoing intake

of nitrogen pollutants. High concentrations of organic and ammonium nitrogen prevented nitrification from occurring. The nitrifying bacteria may be inhibited by the oxygen-consuming organics and poisonous substances present in river water, which could result in an accumulation of ammonium nitrogen. Additionally, due to the high pH of river water, a large concentration of non-ionic ammonium nitrogen was present, which would inhibit the action of nitrifying bacteria and lower nitrification rates. In addition, low river discharge, low SS content, and poor nitrifying bacterial activity contributed to the high ammonium nitrogen level of the river during the dry season.

3.2.3 Turbidity

Sediment frequently tops the list of contaminants or compounds that cause turbidity. Any watershed, however, has a variety of sources for the contaminants or natural elements that can have an impact on the clarity of the water. These can be separated into sources that are caused by humans and by the natural world. Erosion from upland, riparian, stream bank, and stream channel areas are examples of natural sources; however, measurement is challenging because of agriculture and development activity. Erosion can speed up due to human activity. Turbidity is a result of the water becoming coloured by tannic acids, which are frequently found in peat bogs and bog environments. Turbidity can also come from algae that feed on nutrients that enter the stream as a result of leaf breakdown or other naturally occurring decomposition processes. Sediment can also be released by stream channel movement.

Various sources of phosphorus can encourage the growth of algae, which raises turbidity levels. Sources of phosphorus may include bottom sediment, nutrient runoff from other sources, cropland, and wastewater treatment plants. Turbidity may be exacerbated by organic materials from sewage flows, particularly during treatment plant bypasses. Programs to conserve soil and water have long focused on reducing soil erosion on cropland. Urban stormwater runoff from building sites, impermeable surfaces, or other sources is acknowledged as another significant source of silt. In other words, excessive turbidity can negatively affect recreation and tourism by drastically reducing the visual value of lakes and streams. It may raise the price of treating drinking water and food processing water. By diminishing food sources, destroying breeding grounds, and interfering with gill function, it can kill fish and other aquatic species.

4.0 CONCLUSION & RECOMMENDATIONS

In conclusion, our study revealed significant changes as shown in the results in water quality in Selangor rivers throughout time. Nonetheless, it showed positive changes during the pre-pandemic and pandemic lockdown periods. DO, TSS, ammoniacal nitrogen, and turbidity exhibited positive effects on water quality metrics during the pandemic lockdown period, however BOD, COD, and pH levels had increase. To answer the paper's goal, water quality characteristics do have an impact on the COVID-19 pandemic. Because there is no anthropogenic activity during the lockdown period, the positive effects outweigh the bad ones. Despite the positive impact, the turbidity level remains above the Malaysian specified threshold, showing that the average water resources are still polluted in terms of parameters.

Next, pH, ammoniacal nitrogen, and turbidity were the factors that were seen to have significant changes and required more attention. Mitigation and rejuvenation activities are needed in the coming years to ensure improved water supplies, notably for pH, ammoniacal nitrogen, and turbidity, to ensure that these parameters increase to the acceptable level.

In summary, this paper answered the objectives of this paper where the study measured the trend of water quality parameters with the effect of COVID-19 pandemic and identified which parameter was the most significant contributor to contamination in the rivers in Selangor. The study's limitations are that it only focuses on DO, BOD, COD, TSS, pH value, NH_3-NL, and turbidity, and the data provided by DOE only covers the years 2016 to 2020. This paper suggested further attention on the role of policy makers to induce actions towards the needs of safe and clean water resource. This paper also highlight the need of more study towards other water quality parameters and their effects from the COVID-19 pandemic.

5.0 ACKNOWLEDGEMENT

The authors are thankful and highly appreciate the support given by the Department of Environment (DOE), Malaysia for providing the water quality data in this study. The authors would like to acknowledge the financial support from Universiti Tenaga Nasional (UNITEN) under Bold Fund. ■

REFERENCES

[1] Ahmad, S., Kutty, A. A., Raji, F., and Saimy, I. S. (2015). Water Quality Classification Based on Water Quality Index in Sungai Langat, Selangor, Malaysia. Jurnal Teknologi *Sciences & Engineering), 77:30(eISSN 2180-3722), 139–144.

[2] Al-badaii, F., Gasim, M. B., Mokhtar, M. Bin, Toriman, M. E., and Abd Rahim, S. (2021). Water-Pollution Study Based on the Physico-chemical and Microbiological Parameters of the Semenyih River, Selangor, Malaysia. The Arab World Geographer, 15(no 4), 318–334.

[3] Ali, Q., Parveen, S., Yaacob, H., Zaini, Z., and Sarbini, N. A. (2021). COVID-19 and Dynamics of Environmental Awareness, Sustainable Consumption and Social Responsibility in Malaysia. Environmental Science and Pollution Research, 2020. https://doi.org/10.1007/s11356-021-14612-z.

[4] Aman, M. A., Salman, M. S., and Yunus, A. P. (2020). COVID-19 and Its Impact on Environment: Improved Pollution Levels During the Lockdown Period – A Case From Ahmedabad, India. Remote Sensing Applications: Society and Environment, 20(June), 100382. https://doi.org/10.1016/j.rsase.2020.100382.

[5] Aswathy, T. S., Achu, A. L., Francis, S., Gopinath, G., Joseph, S., Surendran, U., and Sunil, P. S. (2021). Assessment of Water Quality in a Tropical Ramsar Wetland of Southern India in the Wake of COVID-19. Remote Sensing Applications: Society and Environment, 23(August), 100604. https://doi.org/10.1016/j.rsase.2021.100604.

[6] Badd. (2020, October 19). Why is Selangor Still Suffering From water Supply Disruptions, Even After 10 Years? CILISOS - Current Issues Tambah Pedas! https://cilisos.my/why-is-selangor-still-suffering-from-water-supply-disruptions-even-after-10-years/.

[7] Bahukhandi, K., Agarwal, S., and Singhal, S. (2020). Impact of Lockdown Covid-19 Pandemic on Himalayan Environment. In International Journal of Environmental Analytical Chemistry. https://doi.org/10.1080/03067319.2020.1857751.

[8] Basheer, A. 0., Hanafiah, M. M., and Abdulhasan, M. J. (2017). A Study on Water Quality From Langat River, Selangor. Acta Scientifica Malaysia, 1(2), 01–04. https://doi.org/10.26480/asm.02.2017.01.04.

[9] Chakraborty, B., Roy, S., Bera, A., Adhikary, P. P., Bera, B., Sengupta, D., Bhunia, G. S., and Shit, P. K. (2021). Eco-Restoration of River Water Quality During COVID-19 Lockdown in the Industrial Belt of Eastern India. Environmental Science and Pollution Research, 28(20), 25514–25528. https://doi.org/10.1007/s11356-021-12461-4.

[10] Chakraborty, B., Roy, S., Bera, A., Adhikary, P. P., Bera, B., Sengupta, D., Bhunia, G. S., and Shit, P. K. (2021). Cleaning the River Damodar (India): Impact of COVID-19 Lockdown on Water Quality and Future Rejuvenation Strategies. In Environment, Development and Sustainability (Vol. 23, Issue 8, pp. 11975–11989). https://doi.org/10.1007/s10668-020-01152-8.

[11] Chakraborty, S., Sarkar, K., Chakraborty, S., Ojha, A., Banik, A., Chatterjee, A., Ghosh, S., and Das, M. (2021). Assessment of the Surface Water Quality Improvement During Pandemic Lockdown in Ecologically Stressed Hooghly River(Ganges) Estuary, West Bengal, India. Marine Pollution Bulletin, 171(July), 112711. https://doi.org/10.1016/j.marpolbul.2021.112711.

[12] Chen, X., Chen, W., Bai, Y., and Wen, X. (2021). Changes in Turbidity and Human Activities Along Haihe River Basin During Lockdown of COVID-19 Using Satellite Data. Environmental Science and Pollution Research. https://doi.org/10.1007/s11356-021-15928-6.

[13] Chowdhury, M. S. U., Othman, F., Jaafar, W. Z. W., Mood, N. C., and Adham, M. I. (2018). Assessment of Pollution and Improvement Measure of Water Quality Parameters Using Scenarios Modeling for Sungai Selangor Basin. Sains Malaysiana, 47(3), 457–469. https://doi.org/10.17576/jsm-2018-4703-05.

[14] Fulazzaky, M. A., Seong, T. W., and Masirin, M. I. M. (2010). Assessment of Water Quality Status for the Selangor River in Malaysia. Water, Air, and Soil Pollution, 205(1–4), 63–77. https://doi.org/10.1007/s11270-009-0056-2.

[15] Gasim, M. B., M. Jamil, M., and Abd Rahim, S. (2009). Water-Quality Assessment of the Langat River at Kilometre 7, Jalan Kajang-Bangi, Selangor, Malaysia. The Arab World Geographer, 12(No 3-4), 188–198.

[16] Giné-Garriga, R., Delepiere, A., Ward, R., Alvarez-Sala, J., Alvarez-Murillo, I., Mariezcurrena, V., Sandberg, H. G., Saikia, P., Avello, P., Thakar, K., Ibrahim, E., Nouvellon, A., El Hattab, O., Hutton, G., and Jiménez, A. (2021). COVID-19 Water, Sanitation, and Hygiene Response: Review of Measures and Initiatives Adopted by Governments, Regulators, Utilities, and other Stakeholders in 84 Countries. Science of the Total Environment, 795, 148789. https://doi.org/10.1016/j.scitotenv.2021.148789.

[17] Hanafiah, M. M., Yussof, M. K. M., Hasan, M., Abdulhasan, M. J., and Toriman, M. E. (2018). Water Quality Assessment of Tekala River, Selangor, Malaysia. Applied Ecology and Environmental Research, 16(4), 5157–5174. https://doi.org/10.15666/aeer/1604_51575174.

[18] Hashim, N. H. F., Mohd Idris, M. A., Abdullah, M., Ahmad Tajuddin, M. F., Jamaluddin, H., Trevor Gunggang, R. A., Muhazeli, M. F., Abdullah, N. S., Karim, J., Mohamed Yusoff, M. A., Hashim, N., and Sharifuddin, S. S. (2018). Water Quality Assessment of the Langat River, Selangor. Malaysian Applied Biology, 47(5), 9–15.

[19] Karunanidhi, D., Aravinthasamy, P., Subramani, T., and Setia, R. (2021). Effects of COVID-19 Pandemic Lockdown on Microbial and Metals Contaminations in a Part of Thirumanimuthar River, South India: A Comparative Health Hazard Perspective. Journal of Hazardous Materials, 416(September 2020), 125909. https://doi.org/10.1016/j.jhazmat.2021.125909.

[20] Khan, R., Saxena, A., Shukla, S., Sekar, S., and Goel, P. (2021). Effect of COVID-19 Lockdown on the Water Quality Index of River Gomti, India, with Potential Hazard of Faecal-Oral Transmission. Environmental Science and Pollution Research, 28(25), 33021–33029. https://doi.org/10.1007/s11356-021-13096-1.

[21] Kour, G., Kothari, R., Dhar, S., Pathania, D., and Tyagi, V. V. (2021). Impact Assessment on Water Quality in the Polluted Stretch using a Cluster Analysis During Pre- and COVID-19 Lockdown of Tawi River Basin, Jammu, North India: An Environment Resiliency. Energy, Ecology and Environment. https://doi.org/10.1007/s40974-021-00215-4.

[22] Lee Goi, C. (2020). The River Water Quality Before and During the Movement Control Order (MCO) in Malaysia. Case Studies in Chemical and Environmental Engineering, 2(May), 100027. https://doi.org/10.1016/j.cscee.2020.100027.

[23] Liu, D., Yang, H., Thompson, J. R., Li, J., Loiselle, S., and Duan, H. (2022). COVID-19 Lockdown Improved River Water Quality in China. Science of The Total Environment, 802, 149585. https://doi.org/10.1016/j.scitotenv.2021.149585.

[24] Mamun, A. A., Hafizah, S. N., Alam, M. Z., Islamic, I., and Gombak, J. (2009). Improvement of Existing Water Quality Index in Selangor, Malaysia. 2nd International Conference on Water & Flood Management (ICWFM).

[25] Muduli, P. R., Kumar, A., Kanuri, V. V., Mishra, D. R., Acharya, P., Saha, R., Biswas, M. K., Vidyarthi, A. K., and Sudhakar, A. (2021). Water Quality Assessment of the Ganges River During COVID-19 Lockdown. International Journal of Environmental Science and Technology, 18(6), 1645–1652. https://doi.org/10.1007/s13762-021-03245-x.

[26] Najah, A., Teo, F. Y., Chow, M. F., Huang, Y. F., Latif, S. D., Abdullah, S., Ismail, M., and El-Shafie, A. (2021). Surface Water Quality Status and Prediction During Movement Control Operation Order Under COVID-19 Pandemic: Case Studies in Malaysia. International Journal of Environmental Science and Technology, 18(4), 1009–1018. https://doi.org/10.1007/s13762-021-03139-y.

[27] Pant, R. R., Bishwakarma, K., Rehman Qaiser, F. U., Pathak, L., Jayaswal, G., Sapkota, B., Pal, K. B., Thapa, L. B., Koirala, M., Rijal, K., and Maskey, R. (2021). Imprints of COVID-19 Lockdown on the Surface Water Quality of Bagmati River Basin, Nepal. Journal of Environmental Management, 289(October 2020), 112522. https://doi.org/10.1016/j.jenvman.2021.112522.

[28] Patel, P. P., Mondal, S., and Ghosh, K. G. (2020). Some Respite for India's Dirtiest River? Examining the Yamuna's Water Quality at Delhi During the COVID-19 Lockdown Period. Science of the Total Environment, 744, 140851. https://doi.org/10.1016/j.scitotenv.2020.140851.

[29] Praveena, S. M., and Aris, A. Z. (2021). The impacts of COVID-19 on the Environmental Sustainability: A Perspective from the Southeast

Asian region. Environmental Science and Pollution Research, March 2020. https://doi.org/10.1007/s11356-020-11774-0.

[30] Qiao, X., Schmidt, A. H., Xu, Y., Zhang, H., Chen, X., Xiang, R., Tang, Y., and Wang, W. (2021). Surface Water Quality in the Upstream-Most Megacity of the Yangtze River Basin (Chengdu): 2000–2019 Trends, the COVID-19 Lockdown Effects, and Water Governance Implications. Environmental and Sustainability Indicators, 10(January), 100118. https://doi.org/10.1016/j.indic.2021.100118.

[31] Santhi, V. A., and Mustafa, A. M. (2013). Assessment of Organochlorine Pesticides and Plasticisers in the Selangor River Basin and Possible Pollution Sources. Environmental Monitoring and Assessment, 185(2), 1541–1554. https://doi.org/10.1007/s10661-012-2649-2.

[32] Sany, S. B. T., Salleh, A., Sulaiman, A. H., Sasekumar, A., Rezayi, M., and Tehrani, G. M. (2013). Heavy Metal Contamination in Water and Sediment of the Port Klang Coastal Area, Selangor, Malaysia. Environmental Earth Sciences, 69(6), 2013–2025. https://doi.org/10.1007/s12665-012-2038-8.

[33] Tokatlı, C., and Varol, M. (2021). Impact of the COVID-19 Lockdown Period on Surface Water Quality in the Meriç-Ergene River Basin, Northwest Turkey. Environmental Research, 197(December 2020), 111051. https://doi.org/10.1016/j.envres.2021.111051.

PROFILES

AINI HIDAYATI SHAHRIR graduated with Bachelor of Civil Engineering (Hons.) from Universiti Tenaga Nasional. She is currently pursuing Master of Engineering (Civil & Environmental) in University of Adelaide. She is a registered Graduate Engineer under the Board of Engineers Malaysia (BEM). Her research interests are Environmental Engineering, Water Resource Engineering and Climate Change.
Email address: aini.hidayati@gmail.com

GASIM HAYDER, PhD, is a Chartered Engineer (CEng) and a senior lecturer at the Universiti Tenaga Nasional (UNITEN). He also served as the Head of Environment and Sustainable Development Cluster, Head of Postgraduate & Laboratory Services Unit in the Institute of Energy and Infrastructure (IEI), Head of Water & Environmental Engineering Unit in the Department of Civil Engineering, and senior researcher for Sustainable Engineering Group at UNITEN. He has several publications, patents and awards in both national and international levels. His research interests are Environmental Engineering, Wastewater treatment, Biological processes, and Solid Waste Management.
Email address: gasim@uniten.edu.my

DEFORMATION RESPONSES OF EXTRUDED ZINC ALLOY

(Date received: 25.08.2022/Date accepted: 12.04.2023)

O. Farayola[1*], M.O. Oyekeye[2], E.F. Ochulor[3], O.P. Gbenebor[4], C.C. Odili[5], S.A. Olaleye[6], S. O. Adeosun[7]

[1,2,6]Department of Mechanical Engineering, University of Lagos*
[3,4,5,7]Department of Metallurgical and Materials Engineering, University of Lagos
[7]Department of Industrial Engineering, Durban University of Technology, Durban, South Africa

[*]Corresponding author: oogodman@gmail.com

ABSTRACT

Severe plastic deformation (SPD) is a technique used to obtain ultra-fine grains (UFGs). However, this technology is expensive and time-consuming. In this study, the conventional deformation technique is used to examine the deformation responses of extruded zinc alloy to achieve fine grain structure by varying die entry angles. Zinc alloy samples were cast into cylindrical billets in sand mould, the samples were machined and tapered at the edge to ease entry into the die for the extrusion process. The die and tools materials were made of mild steel with die entry angles of 15^o, 30^o, 45^o, 60^o, 75^o, and 90^o. Prior to extrusion, the samples were annealed at 400°C because of their hexagonal close-packed (HCP) structure to ease deformation. After annealing, the plastic deformation of alloy samples occurred at 350°C. The extrusion was performed with the aid of a hydraulic press machine that applied pressure on a cylindrical punch and forced the billet through the extrusion die. The results show that the extruded zinc alloy has the highest extrusion stress of 192MPa at 45° die entry angle with fine grains neatly distributed in the matrix and at a 60° die entry angle, the tensile strength and hardness are 177MPa and 95HV respectively with improved ductility. The microstructure of zinc alloy shows equally distributed dendrite-like second-phase intermetallic in the matrix.

Keywords: Annealing, Deformation, Dies, Extrusion, Grain Boundary, Intermetallic

1.0 INTRODUCTION

Extrusion is a manufacturing process that is used in producing profiles such as rods, tubes, and other intricate machine components. Extruded sections find almost infinite uses in all forms of complex shapes in the following areas: automotive, structural, oil and gas, military, medicine, chemical, and nuclear plants. Extrusion is widely applied in non-ferrous fields, especially with alloys of aluminum, copper, magnesium, zinc, etc. Zinc alloy as one of the non-ferrous metals requires manufacturing processes that can achieve fine grain structure useful in medical and structural applications where bio-degradable grain structures are required [1,2,3]. A study on the effect of equal channel angular pressing (ECAP) with four passes on the microstructural and mechanical properties of zinc and zinc alloys with the addition of Ag, Cu, and Mn (0.5wt%) at room temperature reported that the crystallographic structure and grain size are major factors affecting twining morphology in grain refinement [1]. Gokhale *et al*. [2] explored the microstructure and texture evolution of extruded pure zinc under severe plastic deformation (SPD). The study was carried out using indentation scratch at room temperature and a temperature of 150°C. A large grain size reduction from 86μm to (0.6- 2) μm was observed with a basal texture. It has also been affirmed that casting and solidification techniques are good tools in determining the outcome of the microstructural and mechanical properties of cast products. In line with this, an alloy of alumina silicate (Al-9wt. %Si) was studied and the result showed that there is a close relationship between secondary dendrite arm spacing and mechanical properties [3]. The mechanical properties and microstructure were improved when the extrusion was varied. With the increase in extrusion speed from 0.4mm/s to 2.4mm/s and a corresponding increase in elongation from ~3.9% to 12.2% showed complete recrystallisation with an ultrafine grain size of ~0.85μm at lower extrusion speed. However, an increase in extrusion speed produces a well-distributed grain structure having a higher recrystallisation rate [4]. The use of inverse optimisation in the deformation of pure zinc having a poly-crystal structure would produce ultra-fine grains (UFGs) at nano sizes and also give good micro-mechanical properties [5]. In the extrusion of annealed zinc–aluminum alloys where aluminum occurs as slightly coarse grain fibres resulting in good creep properties, high tensile strength, and high ductility to form zinc alumina. A strain rate of 0.034/s and a reduction in percentage elongation from 55% -35% were obtained [6]. The modeling and experimental results of secondary arm spacing revealed the relationship between mechanical properties, microstructure, and solidification parameters of Zn-Al alloy castings.

The secondary arm spacing was discovered as a major factor to stimulate growth rate and solidification time of casting [7].

The microstructural pattern of Al- 9 wt. % Si and Zn-27wt. % Al alloy casting resulted in increasing dendrite arm spacing and decreasing ultimate tensile strength (UTS); the corrosion resistance of the as-cast also increases with increasing dendrite arm spacing. This analysis shows that microstructural pattern affects the mechanical properties of alloys [8]. Piela *et al*. [9] investigated the microstructural and mechanical properties of cast and hot extruded zinc under plastic deformation by conventional extrusion. The mechanical properties of zinc improved with low temperatures having grain refinement that promotes the formation of composite microstructure with hard matrix, forming a soft interconnected structure at the boundary phase. The microstructural manufacturing of Zn-0.8Mg-0.2Sr (wt. %) alloy recorded a minimum grain size of 0.4-0.6μm and a 2.5μm average grain size. The microstructure and grain size structure were found suitable for medical applications [10]. Sztwiertnia *et al*. [11] examined a cyclic change of the deformation path that increases the plasticity of the material and stops the formation and spreading of cracks. This resulted in zinc wires with high mechanical properties and heterogeneous grains structures elongated in the boundary lines. The addition of an alloying element to increase its grain refinement, degree of recrystallisation, and decrease bio-degradation rate was achieved by varying the extrusion speed during the extrusion process. The growth of grains reduces at higher extrusion speed while at lower extrusion speed the grain growth increases as well as the recrystallis ation areas, which improves the mechanical properties of the alloy to a higher degree [12].

In this present study, the effect of varying die entry angles on microstructure and mechanical properties of extruded zinc alloy using mild steel dies in place of conventional tool steel (titanium carbide and diamond) dies were studied.

2.0 EXPERIMENTAL METHOD

The chemical compositions of zinc ingots in Table 1 were derived from spark test analysis. The zinc ingots were placed in a crucible cup for melting using a crucible furnace at 419.5°C. Moreover, the molten metal was poured into the sand mould and gradually allowed to solidify for a few minutes after which the billets were retrieved by the opening of the mould. This was repeated to produce seven cylindrical rods of 400 mm length and 30 mm diameter respectively. The cast samples of zinc were cut approximately to the same size but tapered in front for proper fittings into the die orifice. The cast samples were cleaned and machined into shape as shown in Figure 1 for the extrusion process.

Table 1: Chemical composition of zinc alloy (Extract of Spark test analysis)

Elemental Composition	Percentage Composition (%)
Zn	83.14
Cu	0.46
Fe	0.008
Mn	0.011
Pb	10.57
Cd	0.006
Sn	0.003
Al	5.802

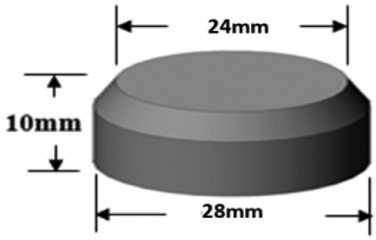

Figure 1: Isometric view of the zinc specimen to be extruded

2.1 Die and Form Tool Materials

Mild steel dies were machined to form a circular end with entry angles of 15°, 30°, 45°, 60°, 75° and 90° as shown in Figure 2. The chemical composition of the mild steel material is shown in Table 2. The mild steel dies were heated and held for 3hrs at 850°C and were subsequently cooled in the furnace to increase the strength of the material. The mild steel form tool and the ram were heated to 850°C and also held for 3hrs with gradual quenching in water. This process was undertaken to increase the strength and hardness of the tools to prevent wear and deformation during extrusion. Figures 2 and 3 show the details of the form tool and ram.

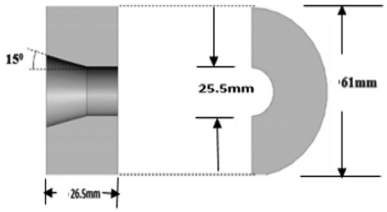

Figure 2: Front view and End view of the die at 15° entry angle

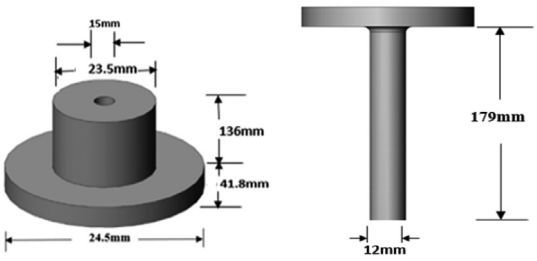

Figure 3: Isometric view of form tool and the schematic diagram of the ram

Table 2: Mild Steel Spectrometer analysis

Elemental Composition	Percentage Composition (%)
C	0.1195
Si	0.2887
S	0.0097
P	0.0099
Mn	0.503
Ni	0.0207
Cr	0.0430
Mo	0.0052
V	0.0065
Cu	0.0312
Fe	98.9

2.2 Extrusion Process

The direct extrusion of the cast samples of zinc alloy was performed using an England Avery Denison machine with identity: (EN76065 7113DCJ), and capacity: 600kN which was adapted for extrusion at ambient temperature to provide a compressive load on the ram. The die was fitted into the form tool and the samples of zinc alloy to be extruded were thereafter inserted through the upper cylindrical part of the form tool. The load (kN) applied on the ram was read alongside the strain gauge attached to the ram of the Avery Denison machine to measure the strain rate. Here, the time taken for the indicator on the strain gauge to complete a revolution was recorded with a corresponding load. Each complete revolution represents a 1mm elongation. The form tool setup was completed by inserting the die into the tool face after which the base was fastened to the container. The sample in Figure 1 was placed into a container through the centre hole and then covered with the ram, thereby completing the extrusion set-up. A compressive load from the punch was applied to the ram by gradually turning down the knob of the extrusion machine, and the ram in turn forced out the samples through the orifice at an extrusion pressure recorded for each sample. The extruded sample showed a reduction in thickness and an increase in length; which was performed by using six samples of zinc alloy at die entry angles of 15°, 30°, 45°, 60°, 75°, and 90° respectively. The extrusion pressures as well as the corresponding strain values were recorded for further analysis as illustrated in Figure 4.

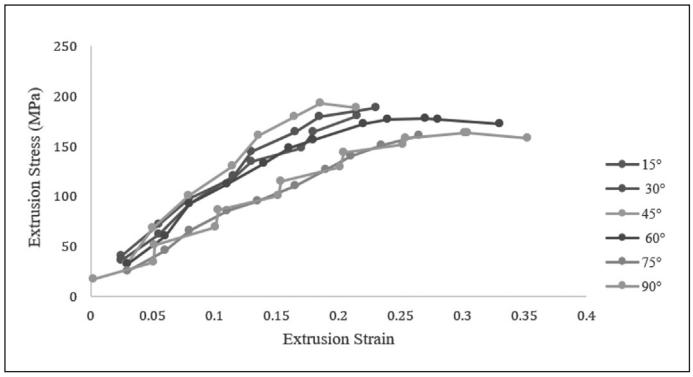

Figure 4: Extrusion stress against Extrusion strain for extruded zinc at varying die entry angles

2.3 Microstructural Examination

The extruded samples of zinc were first rough ground on a bench vice by filing them to an appreciable smoothness and consequently for smooth grinding using 220μ and 600μ emery papers. The smoothened surfaces of these samples were polished to remove scratches obtained during the grinding process. Samples were held on the surface of a polishing machine containing aluminum powder and kept moist by continuous application of waterman. Etching was performed for the 20s using 5g of sodium hydroxide (NaOH) dissolved in 100 mL of water. The etched samples were finally examined on a Celtic metallurgical microscope, model: (S/N: 07035552) at a magnification of X200. The micrographs obtained from Celtic metallurgical microscope were analysed using imageJ software to determine the grain size diameter and count frequency while the origin software was used to analyse the results.

2.4 Hardness Test

A Vickers micro hardness test was performed on Japan-Matsuzawa, model: MMT-X7A, digital micro hardness tester with an applied load of 100gf for a dwell time of 10s. A microscope was attached to the hardness tester to determine the accuracy and the alignment between the indenter and the specimen geometry. Three readings were taken for each sample and the average values were obtained for analysis in Figure 11.

3.0 RESULTS AND DISCUSSIONS

3.1 Extrusion Stress of Zinc Alloy Extruded at Different Angles

The extrusion stresses of zinc alloy extruded at different die entry angles are shown in Figure 4 to be 180MPa, 188MPa, 192MPa, 177MPa, 160MPa and 163MPa at 15°, 30°, 45°, 60°, 75° and 90° die entry angles respectively. The tensile strength of zinc alloy increases as the die entry angle increases to a maximum extrusion stress of 192MPa at 45°; further increase in the die angle leads to a gradual reduction in the extrusion stress of zinc alloy at 90°. The following are the strain values obtained at different die entry angles: 0.215, 0.23, 0.186, 0.27, 0.27 and 0.302. The strain value increases with increase in die angle. However, at 45°, the strain value declines, before it continues to a maximum value of 0.3 at angle 90°. This undulating pattern could be due to non-homogeneity of work hardening of the extrudate. The ductility, strength and hardness of 0.27/177MPa/ 95HV and 0.302/~163MPa/ ~73HV were obtained at 60° and 90°die entry angles respectively. The study observed that extrusion at 60°, 75°, 90° die entry angles enhances zinc alloy ductility. The extrusion stress of 192MPa at die angle 45° was the highest with the lowest extrusion strain of 0.186, while die entry angle 90° recorded the lowest extrusion stress of ~163MPa with the highest extrusion strain of 0.302. The least ductile sample was achieved at 45° die entry angle while samples extruded at 60° and 90° die entry angles showed increase in ductility. This is attributed to the reduction of grain size at higher extrusion speed while at lower extrusion speed the grain size increases, which improves the mechanical properties of the alloy [12].

3.2 Morphology of Zinc Extruded at Different Die Entry Angle

Micrographs of zinc extruded at 15° die entry angle as shown in Figure 5b contains very fine crystals together with the inter-metallic phase. The dendrite-like features of the inter-metallic are dispersed in the grain boundary region and well distributed in the matrix. Figure 5a shows the grain size distribution which gives a fine grain size of 5μm and a maximum bin count frequency of 90Hz. At 30° die entry angle, the zinc matrix in Figure 6b contains fine crystals of the second phase as spiral dendrite features. These dendrites features are interwoven and are well distributed in the matrix. The zinc alloy shows a grain size of 20μm with the maximum frequency of 8Hz in Figure 6a. Also, the zinc matrix at 45° die angle contains dendrite-like features with fine second phase intermetallic that are well distributed in the matrix as shown in Figure 7b. The dendrite-like crystals of the second phase inter-metallic are sandwiched in the matrix.

The secondary dendrite spacing is known to be proportional with dendrite structure and a smaller dendrite spacing, will give a finer structural dendrite morphology [2]. A smaller dendrite secondary spacing improves the mechanical strength of non-ferrous alloy [3,7]. The characteristics of cast structures, having smaller dendrite spacing is mainly due to the shorter wavelength of the periodicity of the micro segregation [7]. Figure 7a gives a grain size of 32.5μm with a frequency of more than 70Hz. The crystals of the zinc matrix in Figure 8b for 60° die angle shows dendritic crystals that are significantly larger in this sample than in Figures 6b and 7b. In Figure 8a, the grain size is 10μm with a maximum frequency of more than 250Hz. Moreover, when the die angle increases to 75° in Figure 9b the result shows more precipitated crystals in the matrix than the results in Figure 8b. However, there is a reduction in the clustering of the inter-metallic phase as well as increase in the fineness of the second phase inter-metallic. In Figure 9a, the grain size is 45μm with a maximum frequency of 110Hz. Figure 10b shows the microstructure of extruded zinc at 90°. Here, there is also an increase in the volume of the second phase precipitated in the matrix, which shows that extrusion at higher angle gives fine HCP structure. The zinc alloy and second phase intermetallic are fine at die angle of 90°, when compared to samples in Figure 10b. Figure 10a gives a grain size of 10μm with a frequency of more than 80Hz.

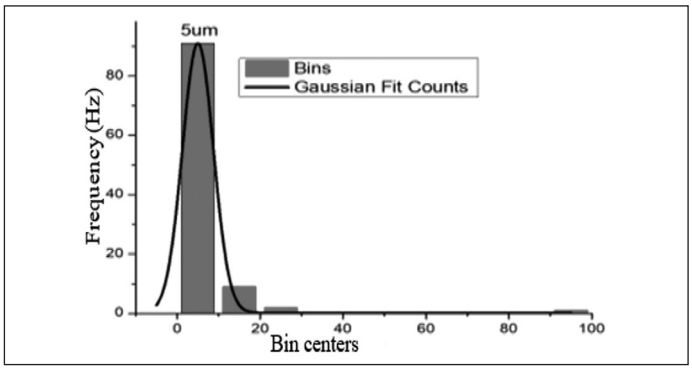

Figure 5a: Count frequency against bin count at 15° die entry angle

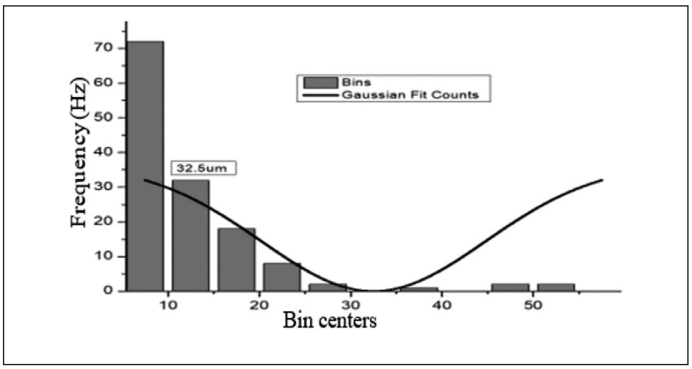

Figure 7a: Count frequency against bin count at 45° die entry angle

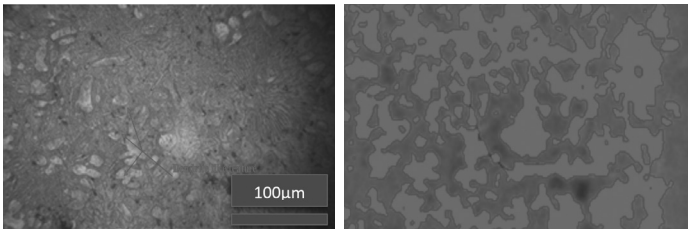

Figure 5b: Micrographs of zinc extruded at 15° die entry angle

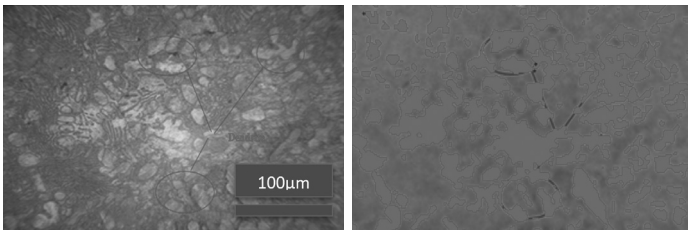

Figure 7b: Micrographs of zinc extruded at 45° die entry angle

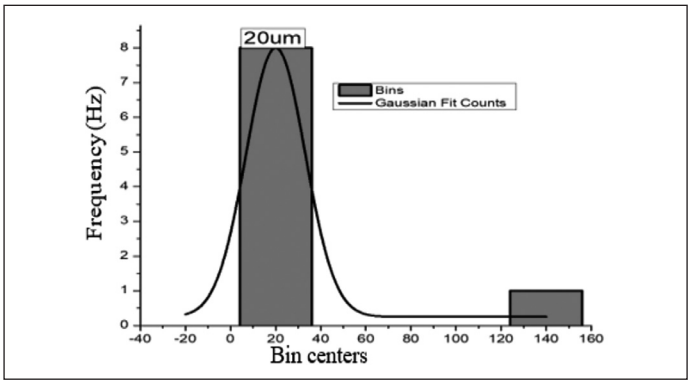

Figure 6a: Count frequency against bin count at 30° die entry angle

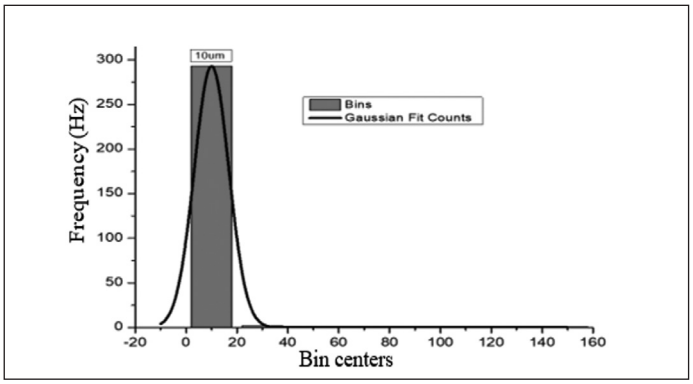

Figure 8a: Count frequency against bin count at 60° die entry angle

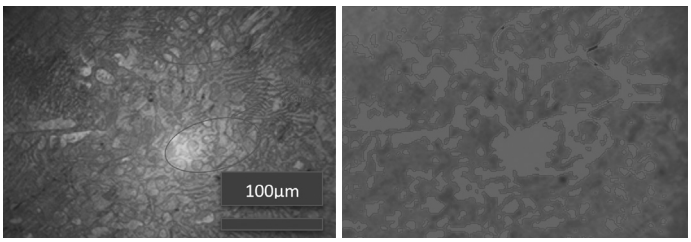

Figure 6b: Micrographs of zinc extruded at 30° die entry angle

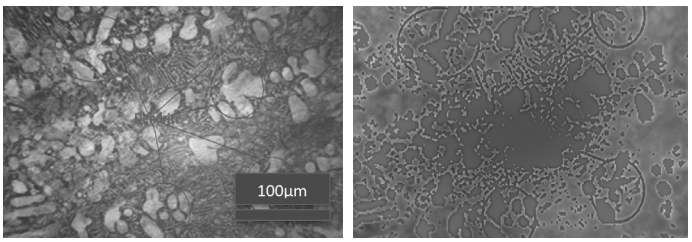

Figure 8b: Micrographs of zinc extruded at 60° die entry angle

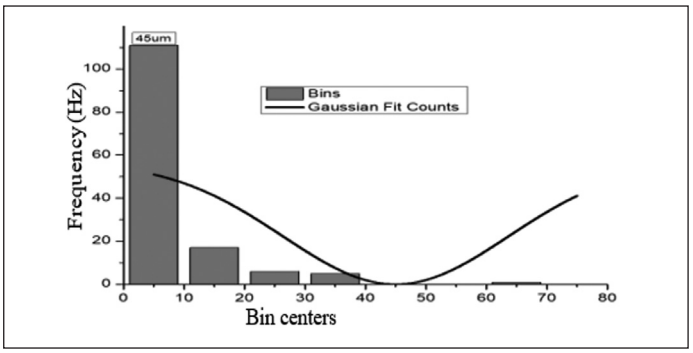

Figure 9a: Count frequency against bin count at 75° die entry angle

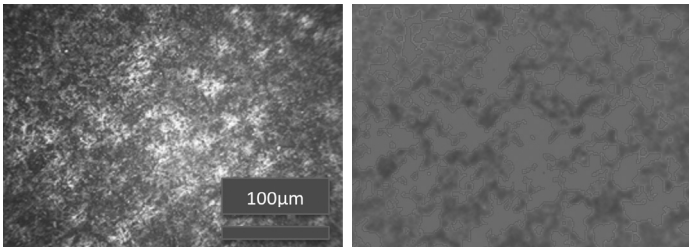

Figure 9b: Micrographs of zinc extruded at 75° die entry angle

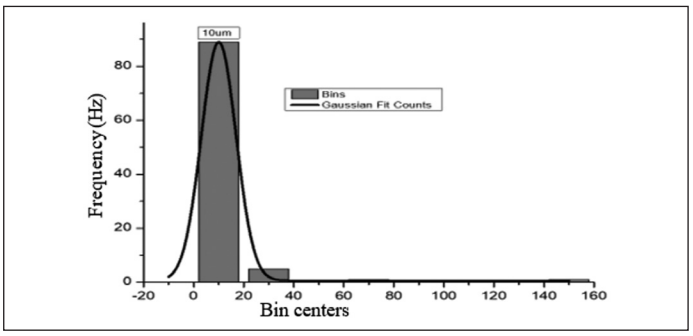

Figure 10a: Count frequency against bin count at 90° die entry angle

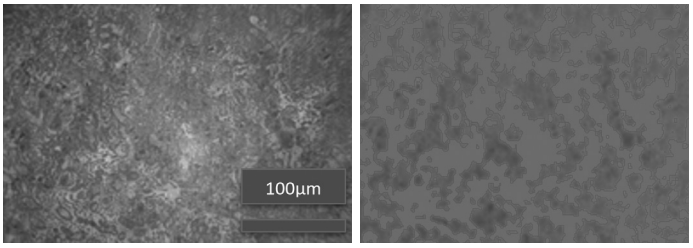

Figure 10b: Micrographs of zinc extruded at 90° die entry angle

3.3 Hardness Features of Zinc Alloy Extruded at Various Die Angles

Hardness test results of the extruded zinc alloys are shown in Figure 11. At die entry angles of 15°, 30°, 45°, 60°, 75°, and 90° with their corresponding hardness values of 85HV, 85HV, 72HV, 90HV, 95HV, and 92.5HV respectively. The zinc alloy shows progressive increase in hardness from 85HV to 95HV between die entry angles of 15° to 60°, before declining to 72HV at 90°. Die entry angle affects the orientation of grains, which appears to align parallel to direction of dislocation motion, thereby relieving the impediment potency along that direction [13]. This enhances grain crystallisation and growth.

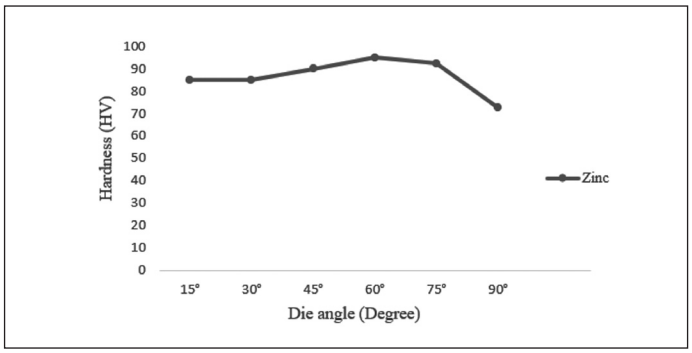

Figure 11: Hardness against die entry angle

3.4 Effect of Extrusion Angle on Ram Speed

The ram velocity decreases with increase in die entry angle when zinc alloys are extruded from 0.2mm/s at 15° to 0.032mm/s at 90°. Between 45° and 90° entry angles, the ram velocity decreases slowly as the value at 45° and 60° are equal in Figure 12. The ram velocity action is dependent on the hardness and strength of the alloy samples, which in turn is a function of the die entry angle and in all, is dependent on the effect of die entry angles on the microstructure of the extruded alloy. Increase in ram speed hinders the growth of grains and as the speed decreases the grain size and recrystallisation increases as recorded in die angles 45°(0.044mm/s), 60°(0.044mm/s), 75°(0.036mm/s) and 90°(0.032mm/s) in Figure 12[4]. It is known that materials with fine grain have proved to improve mechanical properties like hardness, tensile strength, and wear resistance [14]. The hardness and ductility properties of extruded zinc alloy increases with increase in ram speed. The mechanism for these occurrences is traceable to the presence of immobile and mobile dislocations in the alloy matrix respectively. The fragmentation of grain boundaries as a result of the size reduction enhances the dislocation generation, which promotes specimen elongation as the ultimate tensile strength and hardness values increase [15]. At a high ram speed, there is no sufficient time for grain recrystallisation and grain growth, thus forming smaller grain size, which results into improved properties. The result obtained in this research is in agreement with (Kumar *et al*., 2018) [16], reported increase in the tensile strength and surfaced finish of the alloy with increase in ram speed in the study on the effect of ram speed in cold extrusion of nano SIC reinforced 6061 aluminum alloy. The improvement in the property of the extruded alloy was ascribed to strain hardening of the material.

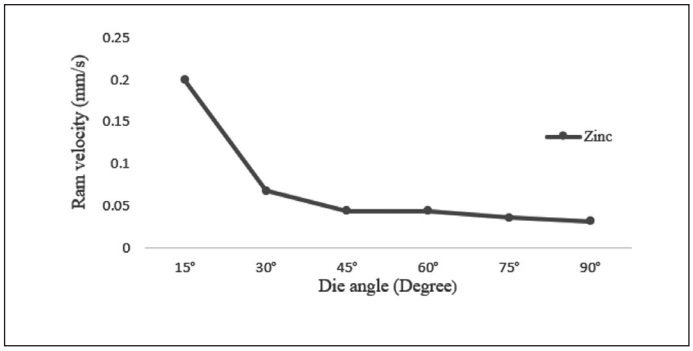

Figure 12: Ram velocity against die entry angle

4.0 CONCLUSIONS

The experimental study conducted on the deformation responses of extruded zinc alloy considering its microstructural and mechanical properties gave the following characteristics:

- The extrusion of zinc gives improved ductility; excellent strength and hardness at 60°extrusion die angle.
- The extrusion ram velocity of zinc alloy decreases with increase in extrusion die angle.
- The use of extrusion at higher die entry angle could be used to help fineness of hexagonal close pack (HCP) alloys.
- This study has shown that aside the use of severe plastic deformation to obtain fine crystals the use of appropriate die entry angle can be utilised to achieve fine crystals.
- Decrease in ram speed increases the texture of microstructure.
- The extrusion at die entry angle of 45° achieved the least ductility with fine texture in the microstructure. ■

REFERENCES

[1] Bednarczyk,W., Watroba, M., Kawalko, J., and Bala, P., (2019) "Can Zinc Alloys be Strengthened By Grain Refinement? A Critical Evaluation of the Processing of Low-Alloyed Binary Zinc Alloys using ECAP," Materials Science and Engineering A 748;357-366 DOI: 10.1016/j.msea.2019.01.117.

[2] Gokhale, A.R., Sarvesha, R., Guruprasad, T. S., Singh, S. S., and Jain, J., (2021) "Tailoring the Surface Microstructure and Texture in Pure Zinc," Materials Science Engineering A 816:141258, Doi: 10.1016/j.mea.2021.141258.

[3] Goulart, P.R., Osorio, W.R., Spinelli, J. E and Garcia, A. (2007). Dendritic Microstructure Affecting Mechanical Properties and Corrosion Resistance of an Al-9wt%Si Alloy. Materials and Manufacturing Processes.22 (3) pp. 328-332.

[4] Li, J., Zhang, A., Pan, H., Ren, Y., Zeng, Z., Hung, Q., Yan, C., Ma, L., and Qin, G. (2020) " Effect of Extrusion Speed on Microstructure and Mechanical Properties of the Mg-Ca Binary Alloy," Journal of Magnesium and Alloys, Elsevier, 2213-9567/ https://doi.org/10.1016/j.jma.2020.05.011. www.elsevier.com / locate/jma, www.sciencedirect.com.

[5] Nguyen, N. P. T., Abbes, F., Abbes, B., and Li, Y., (2018) "Orientation- Dependent Response of Pure Zinc Grains under Instrumented Indentation: Micromechanical Modeling," Proceedings of The International Conference on Advances in Computational Mechanics 2017 (pp157- 169). Doi: 10. 1007/978-981-10-7149-2-11.

[6] Nicholson, S., Meikle, and J. B., (2014) "A Note on Extruded Zinc- Aluminium Alloys," Powder Metallurgy, Metal Technology, Pg 83-88, https://doi.org/10.1179/pom.1966.9.17.006.

[7] Osorio, W.R. and Garcia, A. (2002) "Modeling Dendritic Structure and Mechanical Properties of Zn-Al Alloys as a Function of Solidification Conditions," Material Science and Engineering, A. Volume325, issue1-2, 28th February 2002, Pages 103-111. https://doi.org/10.1016/s0921-5093(01)01455-1.

[8] Osorio, W.R., Goulart, P.R., Garcia, A., Santos, G.A., and Neto, C.M. (2006) "Effect of Dendrite Arm Spacing on Mechanical properties and Corrosion Resistance of Al9(wt.%)Si and Zn 27(wt%) Al alloys", Metallurgical and Materials Transaction, A 37(8): 2525-2538 DOI: 10.10071/BF025862-2-5, Project: Metal Solidification.

[9] Piela, K., Wrobel, M., Sztwiertnia, K., Jaskowski, M., Kawalko, J., Bieda, M., Kiper, M., and Jarzebska, A., (2016) "Zinc Subjected to Plastic Deformation by Complex Loading and Conventional Extrusion: Comparison of the Microstructure and Mechanical Properties," Materilas and Design Volume 117(5 March 2017): 11-120 Doi: 10.10616/j.matdes.2016.12.056.

[10] Pinc, J., Skolakova, A., Vertat, P., Duchon, J., Kubasek, J., Lejcek, P., Vojtech, D., and Capek, J., (2021) "Microstructure Evolution and Mechanical Performance of Ternary Zn-0.8Mg-0.2Sr (wt.%) Alloy Processed by Equal Channel Angular Pressing," Materials Science and Engineering A 824(7): 141809 DOI: 10.1016/j.msea.2021.141809.

[11] Sztwiertnia, K., Kawalko, J., Bieda, M., Jaskowski, M., Piela, K., and Bochniak, W., (2015) "Microstructure and Texture of Zinc Deformed by Extrusion with Forward-Backward Rotating Die(koBo)" IOP Conference Series Materials Science and Engineering 82(1) DOI: 10.1088/1757-899x/82/1/012084.

[12] Wiese, B., Harmuth, J., Willumeit-Romer, R., and Bohlen, J., (2022) "Property Variation of Extruded Mg-Gd Alloys by Mn Addition and Processing," Crystals, MDPI, 2022, 12, 1036, https://doi.org/10.3390/crystal12-081036. www.mdpi.com/journals/crystals.

[13] Adeosun S.O., Sekunowo O.I. and Gbenebor O.P. (2014). Effect of Die Entry Angle on Extrusion Responses of Aluminum 6063 Alloy. International Journal of Engineering and Technology, 4(2), pp 127-134.

[14] Gupta RK, Raman RKS, and Koch CC (2010) Fabrication and Oxidation Resistance of Nanocrystalline Fe10Cr Alloy. J Mater Sci 45: pp 4884–4888.

[15] Balogun, S. A., Esezobor, D. E., and Adeosun, S. O. (2007). Effects of Deformation Processing on the Mechanical Properties of Aluminum Alloy 6063. Metallurgical and Materials Transactions A, USA Volume 38, Pg 1570-1574, July 2007.

[16] Kumar A.J., Lamalasetti, C.H, Ratman, and Kesava Rao V.V.S (2018). A Study on the Effect of Ram Speed in Cold extrusion on the Properties of Nano SiC Reinforced 6061 Aluminum Alloy. International Journal of Mechanical Engineering and Technology. 9(13), pp 1309-1318.

PROFILES

OLANREWAJU FARAYOLA holds a Bachelor's degree in Mechanical Engineering and a Master's degree in Design and production. He is a Ph.D. student in the Department of Mechanical Engineering, University of Ibadan, Ibadan, Nigeria; presently working on grain refinement of bio-aluminum casting using severe plastic deformation method. His research interests are in the areas of materials development, casting, and characterisation.
Email address: oogodman@gmail.com

DR MANASSEH O. OYEKEYE is a Senior Lecturer in the Department of Mechanical Engineering, University of Lagos, obtained the Bachelor of Engineering with Second class honors, Upper division from the University of Ilorin; a Master of Engineering degree from the University of Ibadan and a Ph.D. from the University of Lagos. He is involved in production and maintenance engineering.
Email address: moyekeye@unilag.edu.ng

DR EZENWANYI FIDELIA OCHULOR is a Senior Lecturer at the Department of Metallurgical and Materials Engineering, University of Lagos, Nigeria. She holds a Master's of Science and Ph.D. degree from the same department, and a Bachelor's degree in Engineering from the Federal University of Technology, Owerri (FUTO), Nigeria. Her research interests are materials processing, development, and characterisation. She is currently working on heat treatment processes to reduce carbide precipitates in Thin Wall Ductile Iron (TWDI). Also, her research group is currently working on the development of mannequins for capacity building in Ultrasonography where they are leveraging locally sourced biomaterials for mannequin production.
Email address: eochulor@unilag.edu.ng

DR OLUWASHINA PHILIPS GBENEBOR is a Materials Science and Engineering researcher at the Metallurgical and Materials Engineering Department, University of Lagos, Nigeria. His research is inclined toward the development, processing, and characterisation of materials for engineering applications. He is vast at characterising materials for their thermal, structural, morphological, and mechanical properties. He works on alloys and their properties in areas such as structural modification and strengthening mechanisms. Some research on lignin, cellulose, and chitin from biomass is also being conducted by him. He also develops interests in lignocellulose-soured porous materials for CO_2 capture and energy storage devices.
Email address: ogbenebor@unilag.edu.ng

CLETUS CHIOSA ODILI holds a BEng and MSc in Metallurgical and Materials Engineering. He is a Ph.D. Student in the Department of Metallurgical and Materials Engineering, University of Lagos, Nigeria, working on Biomaterials as Orthopaedic Suture material. His research interests are in areas of materials development and characterisation.
Email address: chiosa.odili@gmail.com

SAMUEL ADEBAYO OLALEYE studied Mechanical Engineering at Yaba College of Technology. He had a passion for research in Engineering and Science fields. He is a Professional Technologist registered with both Nigerian Association of Technologists in Engineering and Council for the Regulation of Engineering in Nigeria. Likewise, he is highly knowledgeable in mechanical instrumentation, automobile, and autotronics (electronics) systems. His objective is to use his experience and skills in giving the organisation he belongs to a competitive edge in the customer service environment. Ready to work with and through others to achieve organisation targets, goals, and objectives to develop a professional career and make positive contributions forthwith.
Email address: solaleye@unilag.edu.ng

PROF. SAMSON OLUROPO ADEOSUN BIO-SKETCH is a Professor of Materials Development, Processing, and Characterisation in the Department of Metallurgical and Materials Engineering, University of Lagos, Nigeria, and has over 150 publications to his credit. He has contributed to Ten book chapters and two full books. He has mentored Eleven PhDs to graduation both nationally and internationally and has five students under supervision both nationally and internationally. He was a visiting scholar at the Chemical Engineering Innovation Group Laboratory, Soochow University Suzhou, China, and at the Department of Chemical, Metallurgical and Materials Engineering, the Tshwane University of Technology Pretoria West campus, Pretoria, South Africa.
Email address: sadeosun@unilag.edu.ng

IOT PLATFORM FOR VITAL SIGNS DETECTION USING NODE MICROCONTROLLER

(Date received: 27.09.2022/Date accepted: 02.05.2023)

Sinan S. Mohammed Sheet[1*], Mohammed S. Jarjess[2], Abdullah K. Shanshal[3], Fatin A. Elhaj [4]

[1,2,3]Northern Technical University, Mosul, Iraq
[4]University of Khartoum, Khartoum, Sudan

[*]Corresponding author: sinan_sm76@ntu.edu.iq

ABSTRACT

Using IoT technology to monitor patients' vital signs can help limit the spread of the coronavirus. Therefore, a cost-effective remote monitoring system measuring vital signs is proposed. Dual heart rate and oxygen level sensor, a temperature sensor, two microcontrollers, UNO as a power supply, and Node as the main controller are used in this system. The vital signs are monitored non-invasively utilising Photoplethysmography equipment and wirelessly relayed to the person involved via the Blynk platform utilising a Wi-Fi device. Photoplethysmography is the core technology for the entire system. It also shows how the system can connect to the internet worldwide, which lets it be used in different clinical tests.

Keywords: Blynk Platform, Internet of Things, Microcontrollers, Vital Signs

1.0 INTRODUCTION

Nowadays, vital signal monitoring systems are essential for identifying various diseases by reading the signal and providing a diagnosis by the appropriate authority, and becoming a crucial requirement in world life [1-4]. The Internet of Things (IoT) health monitoring system is the best solution for monitoring a patient's basic symptoms via an IoT network based on heart rate (HR), oxygen saturation (SpO_2), and temperature sensors as capturing elements, as well as microcontroller as a processing device, as well as a pulse sensor and temperature sensor, from which data is collected and sent to Raspberry PI [5, 6]. However, the major drawback of the system is that no interfaces for data visualization have been created [7]. On the other hand, an excellent integrated device that wirelessly sent a person's pulse to a computer, allowing individuals to test their HR by only looking at their phones rather than needing their hands each time sensing is analysed, was studied [8, 9]. Measurement of vital signs has been integrated into a single device. This study aims to develop and implement a smart, low-cost, and easy-to-use system that monitors a patient's vital activities, including temperature, heart rate, and SpO_2, using unique sensors for each variable and sending readings to the doctor's email and smart phone to keep track of the patient's condition.

2.0 LITERATURE REVIEW

This section describes the most recent scholarly sources on the topic of IoT-based vital sign measurement and monitoring systems. Katoch *et al.,* for example, created a WSN-based health monitoring system that monitors physiological functions in humans [10]. It looked at precautions taken in a potential investigation setting in the course of regular life. In addition, Pinto *et al*. created an Internet of Things-based system to track the health of the elderly. The proposed system's primary functions include data recording and monitoring, as well as the distribution of emergency alerts [11].

Additionally, Li *et al*. presented a healthcare-wide heart disease monitoring system [12]. The system demonstrated effectiveness in addressing the patient's cardiac state once the support mode was switched to the common mode. Healthcare services tailored to the individual's health status are also promoted. An intelligent Internet of Things (Help to You) system was proposed for the elderly by Basanta *et al*. [13]. The project's goal was to enhance the standard of care for the elderly. Jarjees *et al*. have developed another IoT-based system for continuous monitoring of respiratory parameters [14]. It is inexpensive, wearable, and highly reliable.

3.0 METHODOLOGY

This section describes the design and implementation of the hardware and software for the proposed system. Figure 1 illustrates the design and implementation of the hardware. It is evident that all sensors are linked to the main microcontroller (Node Microcontroller). Figure 2 shows the programming flowchart of the proposed system. Heart rate and the SpO_2 value are shown when the switching signal is 1, whereas the temperature reading is shown when the signal is 0. In order to provide power to the board, Arduino UNO Microcontroller contains a USB port. The circuit board is a useful tool for working on electronics projects.

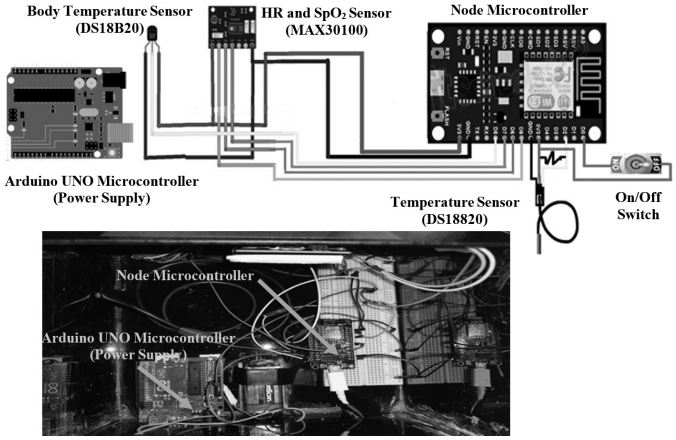

Figure 1: Hardware System Design and Implementation

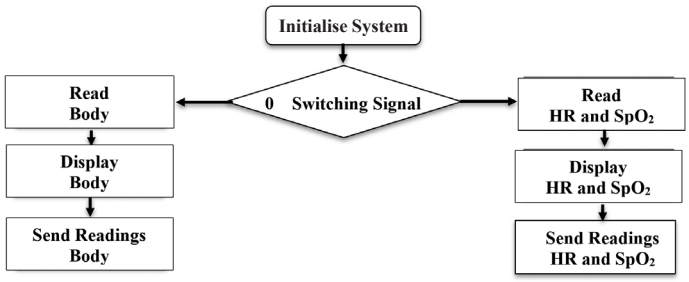

Figure 2: The Flowchart of the Software Program of the Developed System

(a) Proposed System *(b) Conventional Devices*

Figure 3: Comparison Reading

4.0 RESULTS AND DISCUSSION

A Jumper fingers pulse oximeter (model JPD 500E) was utilised to validate the HR and SpO_2 values of the proposed system. Regarding body temperature, a digital pediatric thermometer by Chicco has been utilised. Figure 3 depicts a comparison of the detected values between proposed and conventional systems. Figure 4 is the mobile screen shoots that present the mobile application to display Vital signs and mail box that shows the received mails of Vital signs too. The table 1 illustrates the comparison between the readings of the proposed system (experimental value) and conventional devices (acceptable value). The percent reading error between the proposed system (experimental value) and the conventional devices (acceptable value) have been computed using equation 1. This equation reveals the precision of the proposed technology in comparison to commercial systems. The maximum error computed is less than 4% for all parameters listed as acceptable values.

$$\textbf{Percent } \textit{Error}\ \% = \frac{\textit{accepted value} - \textit{experimental value}}{\textit{accepted value}} \times 100\% \quad (1)$$

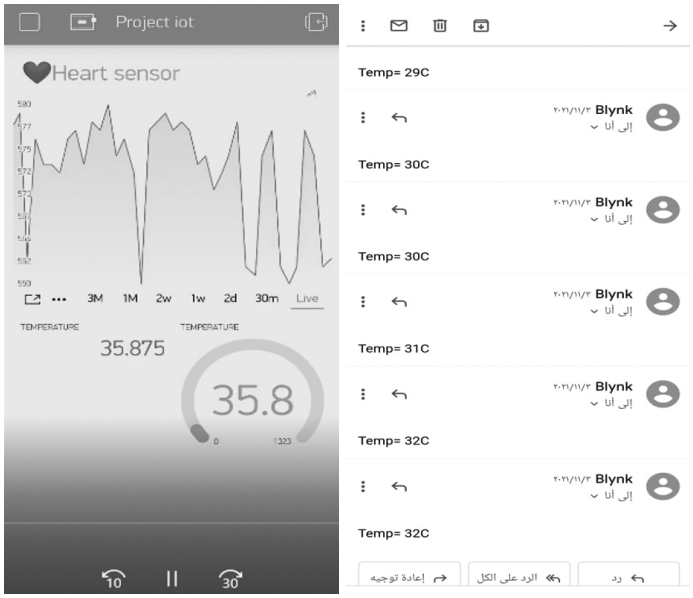

(a) Mobile application displays temperature and heart sensor readings

(b) Mail box shows the received mails that were sent by Arduino

Figure 4: Mobile screen-shoot

Table 1: The Comparison between the Readings of the Proposed system (Pro) and the Conventional Devices (Cd.)

Case No.	Temperature (C°)			Heart rate			SpO_2 rate		
	Cd.	Pro.	Error %	Cd.	Pro.	Error %	Cd.	Pro.	Error %
Case (1)	36.2	36	0.6%	81	81	0.0%	99	96	3.0%
Case (2)	37	36	2.7%	90	88	2.2%	99	96	3.0%
Case (3)	36.4	35	3.8%	92	90	2.2%	99	99	0.0%

5.0 CONCLUSION

The primary objective of the project is to develop and implement a smart, user-friendly, low-cost system that uses specialized sensors to monitor the patient's vital activities (temperature, heart rate, and blood oxygen level) and solves the problem of one reading sent by Blynk platform through the proposed control switching method, then transmits readings to the doctor via the internet (Wi-Fi) to track the patient's condition. The monitoring systems are designed to lower healthcare expenditures, such as the high cost of monitoring patients in hospitals or the cost of keeping track of doctor visits. In compared to commercially available systems, the projected outputs are rather impressive.

Nevertheless, utilising a high-quality sensor may improve accuracy. To further improve the system's response time and decrease measurement errors, a sequential reading technique employing many types of microcontrollers has been integrated into the updated version of the proposed device. ■

REFERENCES

[1] K. K. Nagwanshi *et al.,* "Wearable Sensors with Internet of Things (IoT) and Vocabulary-Based Acoustic Signal Processing for Monitoring Children's Health," Computational Intelligence and Neuroscience, vol. 2022, p. 9737511, 2022/04/28 2022.

[2] M. S. J. Sinan S. Mohammed Sheet, "Microcontroller Based in Vitro Hematocrit Measurement System," Indonesian Journal of Electrical Engineering and Computer Science, vol. 18, No. 2, May 2020.

[3] M. S. A. Sinan S. Mohammed Sheet, "Design and Implementation of Digital Heart Rate Counter by Using the 8051 Microcontroller," 2018 International Conference on Engineering Technologies and their Applications (ICETA), Islamic University – ALNajaf - IRAQ, 2018.

[4] M. Alraja, "Frontline Healthcare Providers' Behavioural Intention to Internet of Things (IoT)-Enabled Healthcare Applications: A Gender-Based, Cross-Generational Study," Technological Forecasting and Social Change, vol. 174, p. 121256, 2022/01/01/ 2022.

[5] S. S. Tamilselvi V, and Vigneshwaran P, "IoT Based Health Monitoring System," 2020 6th International Conference on Advanced Computing & Communication Systems (ICACCS), 2020.

[6] Y. Hagiwara *et al.,* "Computer-Aided Diagnosis of Glaucoma using Fundus Images: A review," Computer Methods and Programs in Biomedicine, vol. 165, pp. 1-12, 2018/10/01/ 2018.

[7] A. S. Tanvi Banerjee "oT Quality Control for Data and Application Needs," iEEE iNTElliGENT SYSTEmS, vol. 17, 2017.

[8] M. M. Islam, A. Rahaman, and M. R. Islam, "Development of Smart Healthcare Monitoring System in IoT Environment," SN Computer Science, vol. 1, no. 3, p. 185, 2020/05/26 2020.

[9] S. Pratikkumar Desai, "Semantic Gateway as a Service architecture for IoT Interoperability," 2015 IEEE International Conference on Mobile Services, 2015.

[10] E. Kańtoch, P. Augustyniak, M. Markiewicz, and D. Prusak, "Monitoring Activities of Daily Living Based on Wearable Wireless Body Sensor Network," (in eng), Annu Int Conf IEEE Eng Med Biol Soc, vol. 2014, pp. 586-9, 2014.

[11] D. Sahu, B. Pradhan, A. Khasnobish, S. Verma, D. Kim, and K. Pal, "The Internet of Things in Geriatric Healthcare," (in eng), J Healthc Eng, vol. 2021, p. 6611366, 2021.

[12] C. Li, X. Hu, and L. Zhang, "The IoT-Based Heart Disease Monitoring System for Pervasive Healthcare Service," Procedia Computer Science, vol. 112, pp. 2328-2334, 2017/01/01/ 2017.

[13] H. Basanta, Y.-P. Huang, and T.-T. Lee, "Intuitive IoT-Based H2U Healthcare System for Elderly People," 2016 IEEE 13th International Conference on Networking, Sensing, and Control (ICNSC), pp. 1-6, 2016.

[14] M. S. Jarjees, M. G. Ayoub, M. N. Farhan, and H. M. Qassim, "Thingspeak-Based Respiratory Rate Streaming System for Essential Monitoring Purposes," Bio-Algorithms and Med-Systems, vol. 16, no. 3, 2020.

PROFILES

SINAN S. MOHAMMED SHEET his Academic Qualifications as follow: The Ph.D. Degree in Biomedical engineering from the University Teknologi Malaysia UTM, Johor, Malausia, in 2022, M. S. Of engineering (Electrical-computer and microelectronic system) University Teknologi Malaysia (UTM) Malaysia, 2011. And a B. Eng. in medical Instrumentation Technology Engineering 1999. Main responsibility: (work as a lecturer at Technical Engineering College, Northern Technical University. Subjects of interest: Biomedical instrumentation, digital image processing, advance digital electronic, microcontroller.
Email address:sinan_sm76@ntu.edu.iq

MOHAMMED S. JARJESS received a PhD in Biomedical Engineering, University of Glasgow, Glasgow, United Kingdom, 2017. Technical Master Degree in Medical Instrumentation Technology Engineering, Technical Engineering College of Mosul, Mosul, IRAQ. 2006. B. Eng. In medical Instrumentation Technology Engineering 2002. Head of Medical Instrumentation Technology Engineering Department, Technical Engineering College of Mosul, Northern Technical University, Mosul, IRAQ. 2017-Now.
Email address: mohammed.s.jarjees@ntu.edu.iq

ABDULLAH K. SHANSHAL received a Bachelor, of Tech. degree in electrical power technology engineering from the Northern Technical University, Engineering Technical College, Mosul, Iraq, in 2005; the M.Tech. degree in electrical power technology engineering from the Northern Technical University, Engineering Technical College, Mosul, Iraq, in 2010. The Ph.D. Degree in electrical engineering from the University of Sheffield, Sheffield, U.K., in 2019. Currently, he is working as a lecturer and researcher at the Northern Technical University, Engineering Technical College. Mosul, Iraq. His current research interests include designing and investigating novel high torque/power density, high efficiency, and low cost.
Email address: a.shanshal@ntu.edu.iq

FATIN AHMED MOHAMMED ELHAJ her Academic Qualifications as follow: PhD. in Computer Science (Specialized in Artificial Intelligent) Universiti Teknologi Malaysia (UTM), Malaysia (2014-2018), MSc. in Computer Science University of Khartoum, Sudan (2008-2009, and BSc. in Computer Science University of Khartoum, Sudan (2000-2005). Research Interests: Image recognition and classification, Digital Signal Processing (EEG, ECG, etc.), Cybersecurity Governance, Emerging Technology (IoT, Blockchain), and Artificial Intelligence, Data Science, Machine Learning and Deep Learning Techniques.
Email address: fatin_elhaj@hotmail.com

FOUNDATION EARTHING SYSTEM – ITS APPLICATION AND ELECTRICAL SAFETY CONSIDERATIONS

(Date received: 23.03.2023/Date accepted: 20.06.2023)

Toh Leong Soon[1*], Leong Kok Wah[2]

[1]Aquarius Engineering Consultants Sdn. Bhd., 31 & 31A, Palma A/3, Seri Palma, Bandar Seri Botani, 31350 Ipoh, Perak, Malaysia

[2]Letrik Seri Pelangi, No. 5, Jalan Lip Seng Onn, Taman Ipoh, 31400 Ipoh, Perak, Malaysia

**Corresponding author: aeceng238@gmail.com*

ABSTRACT

Foundation earthing system greatly reduces the resistance to ground as compared to driven earthing rods. Low resistance to ground is desirable to protect lives – it ensures automatic disconnection of power supply in the event of electrical fault. However, special attention must be given in the application of foundation earthing system to terrace houses and shop lots, where common ground slab steelwork is used throughout the entire row of houses or shop lots. This paper shows the field tests and findings of terrace houses with foundation earthing system, the requirements of the design and installation of foundation earthing system, and the importance of such installation to achieve low resistance to ground, to be able to operate the protective devices for supply disconnection during fault condition.

Keywords: Earth Loop Impedance, Earth Resistance, Equipotential Bonding, Foundation Earthing System, Residual Current Device

1.0 INTRODUCTION

In electrical installations, circuit breakers are used for overload and short circuit protection; and Residual Current Devices (RCDs) are used for leakage current protection. In Malaysia, RCDs shall be installed in accordance with Regulation 36(2), 36(3) and 36(4) of Electricity Regulations 1994. The following formula applies where RCD is used for protection by automatic disconnection of power supply in TT system:

$$R_A \times I_{\Delta n} \leq 50V \quad (1)$$

where:

R_A is the sum of the resistances of the earth electrode and the protective conductor connecting it to the exposed-conductive-parts (in Ohms).

$I_{\Delta n}$ is the rated residual operating current of the RCD.

The electrical installation is depicted in Figure 1. The resistance of the installed earth electrode should be as low as practicable. A value exceeding 200 Ohms may not be stable [1].

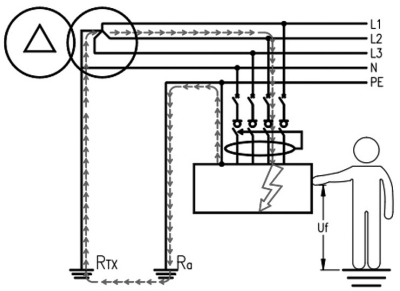

Figure 1: Electrical Installation with Automatic Disconnection of Supply for TT System

The common earth electrode used in electrical installation are:

a. Earthing rods

Earthing rods are vertically driven into the ground. The earthing rods may be copper or more commonly copper-jacketed steel core rods, with screw coupling to reach considerable depth and the desired resistance to ground value. Earth electrode using earthing rods is shown in Figure 2.

b. Foundation earthing system

Foundation steelwork in concrete is used as a readily available and effective earth electrode [2], [3], [4], [5]. The total electrode area formed by the underground steelwork of a structure provides a low resistance to ground value. Foundation earthing system, whereby the earth foundation steelwork is used as earth electrode, is shown in Figure 3.

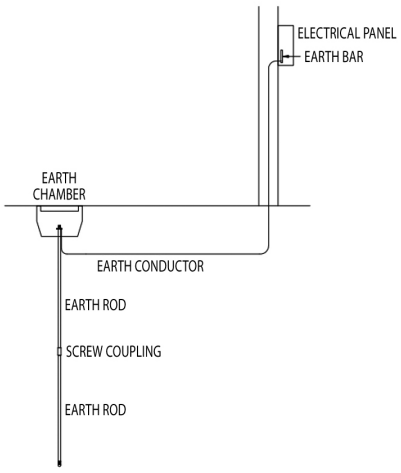

Figure 2: Earth Electrode using Earthing Rods

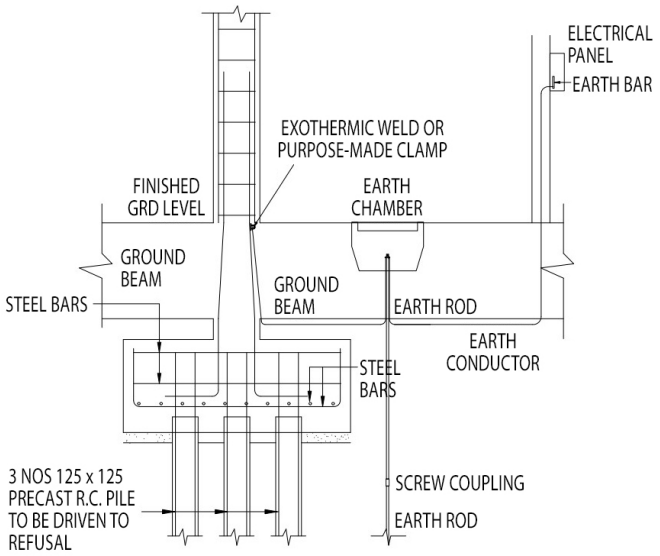

Figure 3: Foundation Earthing System

2.0 FOUNDATION EARTHING SYSTEM – ITS ADVANTAGES AND DISADVANTAGES

Low resistance to ground is essential for automatic disconnection of power supply and safety protection. The question is: what is the resistance to ground value to achieve? Various international and local standards were studied and compared. The recommended resistance to ground value by the various standards is summarised in Table 1.

In order to achieve low resistance to ground value, for instance in Malaysia, equal to or less than 10 Ohms, the earthing rods are installed in parallel, with mutual separation of L to 2L, where L is the driven depth of the earthing rods, as shown in Figure 4.

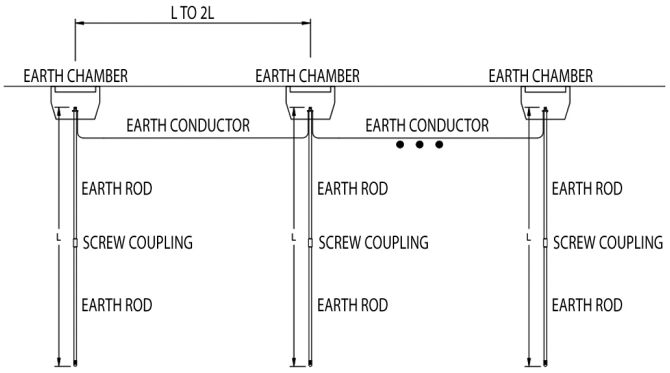

Figure 4: Earthing Rods Installed in Parallel

The effective resistance to ground can be calculated using the following formula:

$$\frac{1}{R_e} = \frac{1}{R_1} + \frac{1}{R_2} + \cdots + \frac{1}{R_n} \quad (2)$$

where:

R_e is the effective resistance to ground (in Ohms).

n is the number of earthing rods installed.

Practically, there is space constraint to install earthing rods in parallel, especially for terrace houses and shop lots. Foundation earthing system provides the solution both technically and economically. The readily available foundation steelwork greatly reduces the resistance to ground value. However, special attention must be given in the application of foundation earthing system to terrace houses and shop lots, where common ground slab steelwork is used throughout the entire row of houses or shop lots.

Table 1: Recommended Resistance to Ground Value by Various Standards

Standard	Recommended resistance to ground value	Remarks
AS/NZS 3000 [6] (Australian/ New Zealand Standard)	Refer to Table 8.1	With reference to earth fault-loop impedance relating to operation of protective devices
BS 7430 [2](British Standard)	1 Ohm	With reference to earth resistance value obtainable with foundation structural steelwork
DIN 18014 [7] (German Standard)	Not stated	In Germany, there is an obligation to erect in every new building a foundation earth electrode according to National Standard DIN 18014
IEEE Std 80 (United States)	IEEE Std 80-2000 [8]: 1 to 5 Ohm	With reference to smaller distribution substations
	IEEE Std 80-2013 [9]: Not stated	Recommended resistance to ground value removed. Resistance value to be estimated by calculation formula.
SS 551 [10] (Singapore Standard)	1 Ohm	With reference to transformer star point earth
	100 Ohm	With reference to operation of RCD
MS IEC 60364-5-54 [5] (Malaysian Standard)	Not stated	-
MS 1936 [3] (Malaysian Standard)	10 Ohms	-
MS 1979 [4] (Malaysian Standard)	10 Ohms	-

In the event of faulty RCD in one of the houses or shop lots, if the fault current is too low for automatic disconnection of power supply by the circuit breaker or the cut-out fuse, the fault current may flow through the foundation earth to other houses or shop lots. The level of touch voltage generated by the fault current could be detrimental to the occupants of the house or shop lot with electrical fault, as well as the other houses or shop lots.

3.0 FIELD TESTS, FINDINGS AND DISCUSSION

To demonstrate the advantages and disadvantages of the foundation earthing system, field tests were carried out at a project site of terrace houses, where foundation earthing system is implemented. The following field tests were carried out:

a. Continuity test on the earth electrode from house to house
   i. Earthing rods without connection to foundation earth
   ii. Earthing rods with connection to foundation earth
b. Earth resistance test using 3-point fall-of-potential earth tester
   i. Earthing rods without connection to foundation earth
   ii. Earthing rods with connection to foundation earth
c. Earth loop impedance test using earth loop tester
   i. Earthing rods without connection to foundation earth
   ii. Earthing rods with connection to foundation earth
d. Simulation of fault condition
   In the event of faulty RCD in one of the houses, check and measure the fault current, the presence of potential touch voltage at the house with electrical fault and other houses, and the effectiveness of automatic disconnection of power supply by the 63A incoming circuit breaker or the 63A cut-out fuse.
   i. Earthing rods without connection to foundation earth
   ii. Earthing rods with connection to foundation earth

The results of the tests are shown in Table 2.

Some of the field test photographs can be found in Figure 5. The field tests and results are illustrated in Figure 6.

(a) Field test set with functional and faulty RCDs for simulation of fault condition

(b) Earth resistance test

(c) Earth loop impedance test - Earthing rods without connection to foundation earth

(d) Earth loop impedance test - Earthing rods with connection to foundation earth

Figure 5: Photographs of Field Tests

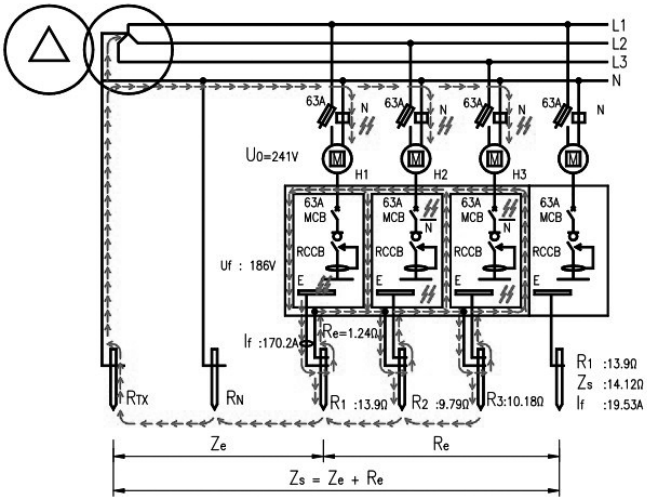

Figure 6: Field Tests and Results

It can be seen from the test results that the earth resistance of earthing rods without connection to foundation earth is generally higher. The earth resistance is greatly reduced with connection to foundation earth. Under the simulated fault condition, i.e. phase to earth fault, with faulty RCD in one of the houses, the fault current is 19.53A for earthing rods without connection to foundation earth (Z_s: 14.12 Ohm). The magnitude of the fault current is not sufficient to trip the 63A incoming circuit breaker. Under the similar fault condition, the fault current is 170.2A for earthing rods with connection to foundation earth (Z_s: 1.54 Ohm). The 63A incoming circuit breaker is tripped off.

For discussion purpose, assuming the effective resistance to ground value of a row of terrace houses or shop lots is 10 Ohm, and the incoming circuit breaker is of 63A. The fault current can be calculated using the following formula:

$$I_f = \frac{U_0}{Z_s} \tag{3}$$

$$I_f = \frac{U_0}{Z_e + R_e} \tag{4}$$

where:

I_f is the fault current
U_0 is the nominal phase to earth voltage
Z_s is the total earth loop impedance
Z_e is the external earth loop impedance
R_e is the effective resistance to ground of the installation

Assuming the external earth loop impedance is very low and negligible. In the event of phase to earth fault, with faulty RCD in one of the houses, the fault current will be:

$$I_f = \frac{U_0}{Z_e + R_e}$$

$$I_f = \frac{230V}{10\Omega}$$

$$I_f = 23A$$

Table 2: Field Test Results

No.	Tests	Results	Remarks
a	**Continuity test**		
i	Earthing rods without connection to foundation earth	H_1 - H_2: 462 Ohm H_1 - H_3: 486 Ohm	
ii	Earthing rods with connection to foundation earth	H_1 - H_2: 0.2 Ohm H_1 - H_3: 0.1 Ohm	
b	**Earth resistance test**		
i	Earthing rods without connection to foundation earth	R_1: 13.9 Ohm R_2: 9.79 Ohm R_3: 10.18 Ohm	
ii	Earthing rods with connection to foundation earth	R_e: 1.24 Ohm	
c	**Earth loop impedance test**		
i	Earthing rods without connection to foundation earth	Z_s: 14.12 Ohm	Prospective Fault Current (PFC): 17A
ii	Earthing rods with connection to foundation earth	Z_s: 1.54 Ohm	Prospective Fault Current (PFC): 157A
d	**Simulation of fault condition**		
i	Earthing rods without connection to foundation earth	I_f: 19.53A	- 63A incoming circuit breaker: no trip - Potential touch voltage at the house with electrical fault: 231.8V
ii	Earthing rods with connection to foundation earth	I_f: 170.2A	- 63A incoming circuit breaker: trip - Potential touch voltage at the house with electrical fault: 186V - Potential touch voltage at the other house: 185V

The magnitude of the fault current is not sufficient to trip the 63A incoming circuit breaker. The fault current will flow to other houses or shop lots through the foundation earth. The RCD of other houses or shop lots will not operate as the fault current is from external and thus not detected by the RCD. The touch voltage generated by the fault current may cause electrocution to the occupants of the house or shop lot with electrical fault, as well as the other houses or shop lots.

The above field tests and discussion show the importance of low resistance to ground in electrical installation, particularly where foundation earthing system is implemented. The required resistance to ground value should be checked against the electrical installation using the following formulas [11]:

$$Z_s = \frac{U_0}{Fusing\ Factor\ \times I_n} \quad (5)$$

where:

Z_s	is the total earth loop impedance
U_0	is the nominal phase to earth voltage
I_n	is the rated current of circuit breaker or fuse
Fusing factor	1.5 for circuit breaker, and 2.4 for fuse

$$Z_s = \frac{U_0}{1.5\ \times I_n \times Earth\ Fault\ setting} \quad (6)$$

where:

Z_s	is the total earth loop impedance
U_0	is the nominal phase to earth voltage
I_n	is the rated current of circuit breaker
Earth Fault Setting	is the percentage setting of earth fault relay, such as 5% and 10%

Formula (5) is used where the protective device is by means of circuit breaker or fuse. Formula (6) is used where the protective device is by means of circuit breaker and protection relay.

4.0 CONCLUSION AND RECOMMENDATIONS

Earth resistance of an electrical installation plays a vital role of safety protection to enable automatic disconnection of power supply in TT system. While foundation earthing system greatly reduces the resistance to ground, special attention must be given in its application, especially in terrace houses and shop lots, where common ground slab steelwork is used throughout the entire row of houses or shop lots. In the event of faulty RCD in one of the houses or shop lots, the magnitude of the fault current shall be sufficient to operate the incoming circuit breaker or cut-out fuse to disconnect the power supply. Otherwise, the fault current may flow through the foundation steels to other houses or shop lots. The level of touch voltage generated by the fault current could be detrimental to the occupants of the house or shop lot with electrical fault, as well as the other houses or shop lots.

Recommendations for the design and installation of foundation earthing system are:

i. Do not merely comply with the recommended resistance to ground value in the Standards. The required value could be lower. Check the required resistance to ground value using Formula (5) or (6) and implement accordingly.
ii. Proper bonding of earthing rods to foundation steel bars shall be ensured. This can be achieved by exothermic weld or purpose-made clamp. Continuity test should be carried out.

The recommended contact resistance is equal to or less than 0.2 Ohm.

iii. Special care should be given on corrosion and oxidation protection - foundation steel bars embedded in concrete provides good corrosion and oxidation protection.

iv. Measure earth loop impedance and Prospective Fault Current (PFC) using earth loop tester as verification of the installation.

v. Periodic inspection and testing. RCDs should be tested at least every 6 months to ensure they are functional.

vi. Design and installation of RCDs in series, with RCD at supply side, and RCDs at load side brand circuits, as per Annex A and Annex B of [4].

5.0 ACKNOWLEDGMENT

The authors wish to acknowledge the project owner for allowing the field tests and findings to be used for discussion in this paper. The authors also wish to thank the competent persons of Persatuan Kekompetenan Penjaga Jentera & Pendawai Elektrik Perak (PKPPE) who have contributed to the field tests, as well as Mr. Ng YT for the Computer Aided Design (CAD) drawing works. ■

LIST OF NOTATIONS

$I_{\Delta n}$ is the rated residual operating current of Residual Current Device
H_1 is the denotation for House 1 of the field tests
H_2 is the denotation for House 2 of the field tests
H_3 is the denotation for House 3 of the field tests
I_f is the fault current
I_n is the rated current of protective device
L is the driven length of earthing rods
R_1 is the resistance to ground for House 1 of the field tests
R_2 is the resistance to ground for House 2 of the field tests
R_3 is the resistance to ground for House 3 of the field tests
R_A is the sum of the resistances of the earth electrode and the protective conductor connecting it to the exposed-conductive-parts
R_a is the resistance of installation earth electrode
R_e is the effective resistance to ground
R_N is the resistance of the supply neutral of overhead poles
R_{Tx} is the resistance of substation transformer neutral earthing
S is the separation distance between earthing rods
U_f is the fault voltage
U_0 is the nominal phase to earth voltage
Z_e is the external earth loop impedance
Z_s is the total earth loop impedance

REFERENCES

[1] BS 7671: 2018 Requirements for Electrical Installations, IET Wiring Regulations Eighteenth Edition, The Institution of Engineering and Technology, pp 63-64, 2018.

[2] BS 7430: 2011+A1: 2015 Code of Practice for Protective Earthing of Electrical Installations, BSI Standards Publication, pp 43-46, August 2015.

[3] MS 1936: 2016 Electrical Installations of Buildings – Guide to MS IEC 60364, Department of Standards Malaysia, pp 49-50, 2016.

[4] MS 1979: 2015 Electrical Installations of Buildings – Code of Practice, Department of Standards Malaysia, p5, p21, 2015.

[5] MS IEC 60364-5-54: 2004 Electrical Installations of Buildings – Part 5-54: Selection and Erection of Electrical Equipment: Earthing Arrangements, Protective Conductors and Protective Bonding Conductors, Department of Standards Malaysia, p19, 2004.

[6] AS/NZS 3000: 2018 Electrical Installations (known as the Australian/New Zealand Wiring Rules), Australian/New Zealand Standard, p427, June 2018.

[7] DIN 18014: 2014 Foundation Earth Electrode – Planning, Execution and Documentation, German Standards, March 2014.

[8] IEEE Std 80-2000 IEEE Guide for Safety in AC Substation Grounding, The Institute of Electrical and Electronics Engineers, USA, p64, January 2000.

[9] IEEE Std 80-2013 IEEE Guide for Safety in AC Substation Grounding, The Institute of Electrical and Electronics Engineers, USA, p66, December 2013.

[10] SS 551: 2009 Code of Practice for Earthing, Singapore Standard, SPRING Singapore, p51, p71, 2009.

[11] Non-Domestic Electrical Installation Safety Code, Energy Commission, Malaysia, p57, 2016.

PROFILES

TOH LEONG SOON is a Professional Engineer with Practising Certificate (PEPC), Member of The Institution of Engineers, Malaysia (MIEM), Qualified Person of National Water Services Commission (SPAN QP), ASEAN Engineer, ASEAN Chartered Professional Engineer (ACPE), APEC Engineer and International Professional Engineer (Int.PE). He received his secondary education from High School Bukit Mertajam, Penang. He obtained his B.Eng (Hons.) and M.Eng from Universiti Teknologi Malaysia in 2003 and 2006 respectively. He has been working as a consulting engineer since 2007 and is currently a Director of a M&E engineering consultant firm in Perak, Malaysia. His area of expertise includes MV and LV electrical system, ELV system, Supervisory Control and Data Acquisition (SCADA) system, motor drives, renewable energy and energy efficiency projects, technical due diligence and building condition assessment.
Email: leongsoon.toh@gmail.com

LEONG KOK WAH is a registered competent chargeman and wireman, with more than 30 years' experience in electrical industry. He is currently a Technical Advisor and Honorary President of Persatuan Kekompetenan Penjaga Jentera & Pendawai Elektrik Perak (PKPPE).
Email address: wah630420@gmail.com

MANUSCRIPT PREPARATION GUIDELINES FOR IEM JOURNAL AUTHORS

The aim of publishing the Journal of the Institution of Engineers Malaysia (or IEM Journal) is to promote the advancement of science, engineering, and technology; disseminate new and current knowledge; share novel findings among practising engineers, researchers and other interested colleagues. Hence, the IEM Journal covers a wide range of practical and diversified engineering disciplines, including publishing papers on any subjects relevant to the engineering and technology of today. As in other journals, all paper submissions to the IEM journal will be peer-reviewed by professionals.

Submission of a contribution is taken to manifest the fact that the submission has not been submitted, accepted, published, or copyrighted elsewhere. To avoid publication delays, please send all manuscripts to the Editor (via the Online Journal Submission) and observe the following guidelines. Each paper is independently peer-reviewed.

Types of Papers

IEM Journal will accept any submissions that fall within the three types of papers shown below:

- **Research Paper**

Significant research and development or applications in any field of engineering and/or technology. Submissions should be about 8-14 pages.

- **Review Paper**

Articles which summarises the state-of-the-art of a specific area of research. Submissions should be about 10-20 pages.

- **Brief Paper**

A concise description of new technical concepts or applications within the scope of the journal. Submission should be about 4 pages

Together with the paper submission, at least four (4) reviewers complete with their contact details (official postal and email address, and telephone number) are to be proposed by authors. Reviewers should be the experts in their research areas.

Plagiarism Policy

IEM Journal strictly prohibits any form of Plagiarism.

If the manuscript has been presented, published, or submitted for publication elsewhere, please inform the Editor. Our primary objective is to publish technical materials not available elsewhere.

Format and Elements of Submitted Texts

a) Initial Submission

For initial submission and reviewing, ALL papers are accepted regardless of the formatting used.

b) Final Submission

Upon final submission of paper, authors are required to follow the manuscript instruction guidelines and paper template as presented below.

Please prepare your main text document in Microsoft Word and PDF format, text should be single line spaced, line numbered and pages should be numbered. You can download the paper template here.

Please note that the style that you submit your paper in (e.g. any additional italics or bold fonts, bullet points, etc.) may be changed on publication to accommodate our publication style.

Manuscript Style

Language:

- The language of the IEM Journal is in English. However, a paper in Bahasa Melayu is also accepted. For accepted papers, an abstract in English and Bahasa Melayu must be included.
- The manuscript should be able to be readily understood by an engineer and researchers alike and should avoid any colloquialisms.
- The terms, including nomenclature and abbreviations, and style should be consistent throughout your journal paper. If you collaborate with other writers, please communicate clearly with them.
- Avoid referring directly to the names of individuals, organisations, products, or services unless essential to the comprehension of the manuscript. Gratuitous flattery or derogatory remarks about a person or organisation should not be included.
- Symbols and Units: SI and derived units should be used, if possible.
- Abbreviations: the use of internationally recognised abbreviations is allowed in the text. The abbreviations should be defined on first use. Abbreviations should not be used in the title.

Manuscript Guide

The following is a detailed manuscript preparation guide for articles submitted to IEM Journal; however, they can, in the most part, be used as a basis for other article types amending to concur with the page limit and premise of the formats, as appropriate.

The manuscript should be typewritten using single-spacing, font of 12 Times Roman; on one side of sheet only and in a single column format.

Title

Titles are limited to 150 characters, including spaces. Please avoid the use of any abbreviations, acronyms, or formulae. Titles should clearly reflect the content of the manuscript and any search terms that readers may use should be considered and incorporated.

List of Authors Name

List down all the names of authors (who has contributed to the paper) and the respective affiliations. From the list of authors, place an asterisk (*) next to the corresponding author's name. Provide an official email address of the corresponding author. **Please DO NOT include your personal telephone number on the title page.**

Abstract

Provide an informative 100 to 250 words abstract at the head of the manuscript. This should be a concise reflection of the aims, findings, conclusions and any interesting or important results. Carefully incorporate any terms that may be used by potential interested readers to improve the article's discoverability online (search engine optimisation). The abstract should contain no reference. Abbreviations that are not commonly used should be defined (for the benefit of the non-specialist reader) at first use.

Keywords

These are used for indexing. Please include between 3-5 keywords.

List of Notations

Please provide a list of symbols and definitions used in the text. This will ease our readers.

Introduction

A concise summary of current background knowledge, with reference to relevant previous works in the field should be presented. Please also describe the objectives of and justification for the work contained in the submitted manuscript.

Main Text

The methods and processes applied to investigate and achieve the objectives should be communicated in sufficient detail that readers could repeat the work successfully. The results should be reported clearly and interpreted accurately and analysed thoroughly. Figures/tables can be used to support these results.

It is important that all research articles include a section at the end of the main text that highlights the novelty of the results to the engineering field and any potential applications.

All sections should be numbered in Arabic such as 1, 2, etc. with the title in capitals. Sub-sections should be numbered such as 1.1, 2.3, etc. Numbered all equations in round brackets ( ) flush to the right. The equation should be in the centre.

Style for Illustrations (Tables and Figures)

Try to include the illustrations in between the text. Each illustration must be numbered such as "Figure 1, Figures 2-3, etc." and have a meaningful caption at the bottom. For tables, the caption must be at the top.
On graphs, show only the coordinate axes, or at most the major grid lines, to avoid a dense hard-thread result.

All lettering should be large enough to permit legible reduction of the figure to column width. Typing on figures is not acceptable. Photographs should be glossy prints, of good contrast and gradation and any reasonable size.

Conclusions

A concise summary of the results of case studies or research project papers and the lessons learned should be discussed. If necessary, please elaborate the applicability / relevance of your article to readers in other countries.

Research journals must discuss the practical relevance and potential applications of the engineering work described. This is important to readers working in engineering related practice.

Please also include relevant references to demonstrate how previous engineering research work has been used. These references could be standards, codes or relevant past journal papers.

Appendices

Additional information, such as tables or mathematical derivations can be included. These will be included in the article.

Acknowledgements

Please provide acknowledgement details to those persons or organization that contributed to the paper. Additional details required by funding bodies can be included.

References

The references to other literature that you have cited in your main text should be based on the APA style of referencing (Author, Date) as described below. Please refer https://apastyle.apa.org/ for a detailed guide on the referencing style.

- Single author: (Author, Year) or Author (Year)
- Two authors: (Author 1 & Author 2, Year) or Author 1 and Author 2 (Year)
- Three and more authors: (Author 1 et al., Year) or Author 1 et al. (Year)

In the text, the author and year of the reference should be put in parentheses immediately after the work referred to, for example 'Controlled tests on the Millennium Bridge (Chapman et al., 2005; Murray & Geddes, 1987; Wilby et al., 2011) during which.....' or 'as mentioned by Lim et al. (2018), the NCA derived from the agricultural wastes...'

All references must be listed, in full, at the end of the paper in alphabetical order, irrespective of where they are cited in the text.

In the reference section, the references should be written in full, as follows:

Books: Author 1 surname, author 1 initials, & Author 2 surname, author 2 initials. (Year of publication). Book title. Publisher, City, Country. doi reference. For example:

Kobayashi, K., Khairuddin, A. R., Ofori, G. & Ogunlana, S. (Eds.). (2009). *Joint ventures in construction*. Thomas Telford, London, UK.

Owen, G. & Totterdill, B. (2008). *The dispute board hearing. In Dispute Boards: Procedures and Practice*. Thomas Telford, London, UK.

Journal, magazine and newspaper articles: Author 1 surname, author 1 initials, & Author 2 surname, author 2 initials. (Year of publication). Paper title. Journal title, Volume (Issue number), First page-Last page. doi reference. Unpublished papers and theses should not be cited as they are not readily available.

Lim, J. L. G., Raman, S. N., Lai, F. C., Zain, M. F. M., & Hamid, R. (2018). Synthesis of nano cementitious additives from agricultural wastes for the production of sustainable concrete. *Journal of Cleaner Production*, 171, 1150-1160. https://doi.org/10.1016/j.jclepro.2017.09.143.

Soon, F. C., Khaw, H. Y., Chuah, J. H., & Kanesan, J. (2018). Hyper-parameters optimisation of deep CNN architecture for vehicle logo recognition. *IET Intelligent Transport System*, 12(8), 939-946. https://doi.org/10.1049/iet-its.2018.5127.

Conference proceedings: Author 1 surname, author 1 initials, & Author 2 surname, author 2 initials. (Year of publication). Paper title. Proceedings title, Volume (Issue number), First page-Last page. doi reference. Unpublished conference proceedings (i.e. that were only given to delegates) should not be cited as they are not generally available.

Chuah, J. H., Khaw, H. Y., Soon, F. C., & Chow, C. (2017). Detection of Gaussian noise and its level using deep convolutional neural network. *Proceedings of the TENCON 2017 - 2017 IEEE Region 10 Conference*, 2447-2450. https://doi.org/10.1109/TENCON.2017.8228272.

Unpublished material should not be included in the Reference list.

Please refer to https://apastyle.apa.org/ for a detailed guide on the referencing style. Authors should strictly adhere to the referencing style specified herein.

Mathematical Equations

Only relevant equations should be included in the main text and should be numbered. An equation editor program can be used to type in a formula.

Figures and tables caption list: Please supply a figure caption list at the end of your journal paper. Figures and tables must be put in the text in consecutive order. All figures must have a brief title accompanied with a short description.

Brief Profile

At the end of the manuscript, each author should provide a brief profile (less than 150 words), together with recent photographs (preferable less than 3 MB).

Corresponding Authors

We only permit one corresponding author per submission.

Conflict of Interest

Conflict of interest occurs when an author (or the author's institution) has personal or financial relationships that inappropriately influence the statements in the publication. Authors should ensure that publications will be written in an unbiased, ethical and responsible manner. The authors working on any sponsored engineering work or publications should declare such work under Conflict of Interest during submission.

Submission of Paper

Authors are required to submit via the IEM Online Journal Submission (OJS) through the following link:

https://iemjournal.com.my/index.php/iem/about/submissions.

Together with the manuscript, the corresponding author should enclose a cover letter containing the significance of the paper, the postal and email address, and telephone number for correspondence. In the cover letter, kindly provide four (4) names as reviewers. The selected reviewers must have the relevant knowledge and research experience. Provide the reviewers postal and email addresses and telephone numbers (if possible).

Further Enquiries

For further enquires, please contact Secretariat at the address shown below:

The Institution of Engineers, Malaysia
Bangunan Ingenieur, Lots 60 & 62, Jalan 52/4
Peti Surat 223 (Jalan Sultan), 46720 Petaling Jaya, Selangor Darul Ehsan
Tel: 03–79684001/2 Fax: 03–79577678
E-mail: pub@iem.org.my or iemjournal@gmail.com

ADVERTISING
To advertise in Journal of IEM, please contact Dimension Publishing Sdn. Bhd. Advertisements that appear in Journal of IEM implies neither endorsement nor recommendation by The Institution of Engineers, Malaysia.

SUBSCRIPTIONS
To subscribe Journal of IEM please contact Dimension Publishing Sdn. Bhd.

DIMENSION PUBLISHING SDN. BHD.
Level 18-01, PJX-HM Shah Tower,
No. 16A, Persiaran Barat,
46050 Petaling Jaya,
Selangor Darul Ehsan, Malaysia.
Tel : (603) 7493 1049
Fax: (603) 7493 1047
Email: info@dimensionpublishing.com

The Institution of Engineers, Malaysia

Bangunan Ingenieur, Lots 60/62, Jalan 52/4, Peti Surat 223 (Jalan Sultan), 46720 Petaling Jaya, Selangor Darul Ehsan
Tel : 03-79684001/2 Fax : 03-79577678 E-mail : sec@iem.org.my IEM Homepage: http://www.iem.org.my

REFEREES FOR VETTING OF IEM PUBLICATIONS

Dear IEM Members/Readers,

The Standing Committee on Information and Publications is revising the list of referees to assist in the vetting of articles received from members and non-members. The referees should preferably be at least Corporate Members of The Institution or graduates with higher degrees.

The aim of appointing the referee is to ensure and maintain a standard in the IEM Publications namely the bulletin and the Journal.

Members who are interested to be placed in the database of referees are to return the registration form to the IEM Secretariat, providing details of their degrees and particular expertise and experience in the engineering fields.

We need your services to look into the vetting of articles received for Publications and due acknowledgement would be announced yearly in the Bulletin. Referees must be committed to return the papers within a month from date of appointment.

Chairman
Standing Committee on Information and Publications

All correspondences are to be addressed to: -

The Chief Editor
Standing Committee on Information and Publications
The Institution of Engineers, Malaysia
Bangunan Ingenieur, Lots 60 & 62, Jalan 52/4
P.O. Box 223 (Jalan Sultan)
46720 Petaling Jaya
Selangor Darul Ehsan

AREAS OF INTEREST FOR VETTING OF PAPERS

Please tick (√) the appropriate area of interest that you are able to vet the papers.

□ Acoustics
□ Engineering Education
□ Military Vehicles
□ Room Temperature
□ Aerodynamics
□ Environmental Engineering
□ Mini Pressure Meters
□ Safety Engineering
□ Air Conditioning
□ Fine Chemical
□ Mining Engineering
□ Scaffolding Works
□ Air Pollution Control
□ Finite Element
□ Naval Architecture
□ Seepage
□ Aircraft
□ Fire Detection
□ Navigation
□ Sewerage
□ Airport Engineering
□ Fire Engineering
□ Oil & Gas Engineering
□ Shipbuilding
□ Aluminium Design
□ Floods
□ Operation Research
□ Signal Processing
□ Arbitration
□ Food Processing
□ Palm Oil Industries
□ Solar Energy Technology
□ Automation
□ Foundation Engineering
□ Petrochemicals
□ Steelworks Design
□ Automotive Engineering
□ Fuzzy Logic
□ Petroleum Engineering
□ Stream Turbine Power Plant
□ Biochemical Engineering
□ Gas Engineering
□ Pharmaceuticals
□ Sructural Analysis
□ Biotechnology
□ Geotechnical
□ Piling
□ Structural Rehabilitation
□ Boiler Engineering
□ Heat Exchanger
□ Plumbing Engineering
□ Survey Engineering
□ Bridge Engineering
□ Highway
□ Pollution Control
□ Taligates
□ Building Services
□ Hydraulics
□ Ports & Harbour Engineering
□ Telecommunication
□ Coastal Engineering
□ H.V. Electrical Distribution
□ Power Electronics
□ Thermal Engineering
□ Co-Generation
□ Industrial Engineering
□ Power Generation
□ Timber Design
□ Computer Engineering
□ Industrial Transport
□ Pressure Vessels
□ Tool Engineering
□ Concrete Design
□ Industrial Ventilation
□ Prestressed Concrete
□ Transfer Tunnels
□ Concrete Technology
□ Information Technology
□ Project Management
□ Transportation Engineering
□ Construction Management
□ Instrumentation
□ Public Administration
□ Urban Planning
□ Control Engineering
□ Lighting System
□ Public Health Engineering
□ Vehicles
□ Drainage Engineering
□ L.V. Electrical Distribution
□ Quarry Engineering
□ Vertical Transportation
□ Dynamics Design
□ Manufacturing
□ Railways
□ Waste Treatment
□ Earthworks
□ Mass Transit
□ Reclamation Works
□ Waste Water
□ Edible Oil Refining
□ Mechanical Handling Equipment
□ Refrigeration
□ Water Resources Engineering
□ Electrical Transmission
□ Management
□ Reinforced Concrete Beams
□ Water Pollution Control
□ Electrochemical
□ Metal Fabrication
□ Road Transport
□ Wind Engineering
□ Electrotechnology
□ Metallurgy
□ Robotics
□ Others (please specify)
□ Energy Technology
□ Micro Electronics
□ Roof Structures

DISCIPLINES / SUB-DISCIPLINES OF VETTER

Please tick (√) the appropriate boxes.

□ Aerospace
□ Electrical
□ Marine
□ Petroleum
□ Aeronautical
□ Electronics
□ Mechanical
□ Production
□ Agricultural
□ Environmental
□ Mining
□ Structural
□ Chemical
□ Industrial
□ Naval Architecture
□ Others (Please specify)

VETTER'S DETAILS

Name : _____
Membership No. : _____ *(if applicable)*
Grade : ☐ Graduate ☐ Member ☐ Fellow ☐ Affiliate ☐ Others
(please specify) _____
Qualifications : _____
Addresses : *(Office)* _____
_____
(Residence) _____
_____
Contact No. : _____ *(Handphone)* _____ *(Office)* _____ *(Residence)*
E-mail Address : _____

Please mail all correspondences to the below. Please tick (√) the appropriate boxes.
Mail to : ☐ Office ☐ Residence

Brief Biodata (not longer than 50 words) (to be appended with this Reply Slip).
_____
_____
_____
_____
_____

Have you ever reviewed submissions for publication in any Journal(s) before? ☐ Yes ☐ No
If YES, name the Journal(s) _____

Do you have papers published in any Journal(s)? ☐ Yes ☐ No
If YES, name the Journal(s) _____

Date: _____ Signature : _____

INTERNATIONAL ADVISORY PANEL FOR IEM JOURNAL

IEM BRANCHES

HEADQUARTERS	**THE INSTITUTION OF ENGINEERS, MALAYSIA** Bangunan Ingenieur, Lots 60/62, Jalan 52/4, P.O.Box 223, (Jalan Sultan), 46720 Petaling Jaya, Selangor	Tel : 03-7968 4001 / 4002 Fax : 03-7957 7678 sec@iem.org.my www.myiem.org.my
PENANG	**IEM PENANG BRANCH SECRETARIAT** 1-04-02 E-Gate, Lebuh Tunku Kudin 2, 11700 Gelugor, Pulau Pinang	Tel : 04-606 599 iempenangbranch@gmail.com http://iempenang.org
SOUTHERN	**IEM SOUTHERN BRANCH SECRETARIAT** 24-B, Jalan Abiad, Taman Tebrau Jaya, 80400 Johor Bahru, Johor Darul Takzim	Tel : 07-331 9705 Fax : 07-331 9710 iemsouthern@gmail.com www.iemsb.org.my
PERAK	**IEM PERAK BRANCH SECRETARIAT** No. 60B, Jalan Lapangan Siber 1, Bandar Cyber (Business Centre), 31350 Ipoh, Perak Darul Ridzuan	Tel : 05-313 8459 iemperakbranch@gmail.com
EASTERN	**IEM PAHANG BRANCH SECRETARIAT** Ketua Penolong Pengarah Kanan Elektrik, JKR Cawangan Elektrik, Jalan Kamunting 2, Seri Kemunting, 25100 Kuantan, Pahang	Tel : 09-513 3533 Fax : 09-514 1594 mazman@jkr.gov.my
TERENGGANU	**IEM TERENGGANU BRANCH SECRETARIAT** 23-05, KT Business Centre, Padang Hiliran, Jalan Sultan Mohamad, 21100 Kuala Terengganu	Tel : 09-620 4500 Fax : 09-620 4502 iemterengganu@gmail.com
NEGERI SEMBILAN	**IEM NEGERI SEMBILAN BRANCH SECRETARIAT** No. 77-A-1, Lorong Haruan 5/3, Oakland Commerce Square, 70300 Seremban, Negeri Sembilan	Tel : 06-631 1011 Fax : 06-631 4619 iemnsembilan@gmail.com www.iemns.org.my
MELAKA	**IEM MELAKA BRANCH SECRETARIAT** C/O Sri Perunding Consulting Engineers, No. 2, Jalan Malinja 2, Taman Malinja Bukit Baru, 75150 Melaka	Tel : 06-284 8028 Fax : 06-283 8919 spcesb@gmail.com
SARAWAK	**IEM SARAWAK BRANCH SECRETARIAT** International Engineering Centre (IntEC), A2-G-19 & A2-1-19, Isthmus Raintree Square, Lot 3249, MTLD Block 7, Jalan Keruing, 93450 Kuching, Sarawak	Tel : 082-288 856 Fax : 082-288 856 iemsarawak@gmail.com
SABAH	**IEM SABAH BRANCH SECRETARIAT** Lot 25, 3rd Floor, Block C, Damai Point Commercial Centre, Lorong Damai Point, Off Jalan Damai, 88100 Kota Kinabalu, Sabah	Tel : 088-259 122 Fax : 088-236 749 iemsabah@gmail.com www.iemsabah.org.my
MIRI	**IEM MIRI BRANCH SECRETARIAT** 2nd Floor, Unit 14 (906-3-14), Soon Hup Tower Complex, (Mega Hotel), Jalan Merbau, 98000 Miri Sarawak	Tel : 085-423 718 Fax : 085-424 718 iem.miri@gmail.com www.iem-miri.org.my
KEDAH / PERLIS	**IEM KEDAH/PERLIS BRANCH SECRETARIAT** No. 164, Tingkat 2, Kompleks Alor Setar, Lebuhraya Darul Aman 05100 Alor Setar, Kedah Darul Aman	Tel : 04-734 3420 Fax : 04-733 3962 iemckps@gmail.com
PAHANG	**IEM PAHANG BRANCH SECRETARIAT** No. 114, Block F, Lorong Seri Teruntum, Medan Warisan, 25100 Kuantan, Pahang Darul Makmur	Tel : 019-855 6509 Fax : 09-514 6493 iempahang@gmail.com
KELANTAN	**IEM KELANTAN BRANCH SECRETARIAT** Lot 5139, Kompleks Niaga INOtrus Kawasan Perindustrian Pengkalan Chepa II, 6100 Kota Bharu, Kelantan	Tel : 09-773 0899 Fax : 04-733 3962 iemckps@gmail.com

IEM
The Institution of Engineers, Malaysia

THE INSTITUTION OF ENGINEERS, MALAYSIA
Bangunan Ingenieur, Lots 60 & 62, Jalan 52/4,
P.O. Box 223 (Jalan Sultan),
46720 Petaling Jaya, Selangor Darul Ehsan.

Tel: 03-7968 4001/4002
Fax: 03-7957 7678
E-mail: sec@iem.org.my
Homepage: http://www.myiem.org.my